American Mineralogist, Volume 70, pages 1270–1289, 1985

Thermodynamic properties of tetrahedrite-tennantites: constraints on the interdependence of the Ag⇌Cu, Fe⇌Zn, Cu⇌Fe, and As⇌Sb exchange reactions

RICHARD OLMSTED SACK AND ROBERT R. LOUCKS

Department of Geosciences
Purdue University
West Lafayette, Indiana 47907

Abstract

Experimental constraints, petrologic studies, and theoretical analysis suggest that, energetically, tetrahedrite-tennantite sulfosalts are remarkably well behaved multisite reciprocal solutions. Fe–Zn exchange experiments (500°C) between tetrahedrite-tennantite and sphalerites yield values of 2.59 ± 0.14 and 2.07 ± 0.07 kcal/gfw for the Gibbs energies of the reciprocal reaction

$$Cu_{10}Zn_2Sb_4S_{13} + Cu_{10}Fe_2As_4S_{13} = Cu_{10}Fe_2Sb_4S_{13} + Cu_{10}Zn_2As_4S_{13}$$

and Fe–Zn exchange reaction

$$1/2\ Cu_{10}Fe_2Sb_4S_{13} + ZnS = 1/2\ Cu_{10}Zn_2Sb_4S_{13} + FeS, \text{ respectively.}$$

These results, plus petrologic studies of tetrahedrite-tennantite + sphalerite assemblages, and preliminary experimental results at 435 and 365°C suggest that the above parameters are insensitive to temperature and permit estimates for the Gibbs energies of the remaining two reciprocal reactions of "ideal" tetrahedrite-tennantite ($(Ag,Cu)_6Cu_4(Fe,Zn)_2\ (As,Sb)_4S_{13}$): $Cu_{10}Zn_2Sb_4S_{13} + Ag_6Cu_4Fe_2Sb_4S_{13} = Cu_{10}Fe_2Sb_4S_{13} + Ag_6Cu_4Zn_2Sb_4S_{13}$ and $Ag_6Cu_4Fe_2Sb_4S_{13} + Cu_{10}Fe_2As_4S_{13} = Cu_{10}Fe_2Sb_4S_{13} + Ag_6Cu_4Fe_2S_{13}$ of 3.0 ± 1.5 and 17 ± 5 kcal/gfw, respectively.

These considerations suggest that tetrahedrite-tennantites are the "Cadillac" of reciprocal solutions and of petrogenetic indicators of hydrothermal mineralizing environments; they are the sulfide analog of amphiboles, the "Rolls Royce" of reciprocal solutions and petrogenetic indicators. In addition to providing a means for deducing aspects of the chemistry of many hydrothermal mineralizing fluids, our results afford an improved basis for understanding downstream chemical zoning in polymetallic base-metal sulfide and bonanza precious metal deposits. In particular they provide strong evidence that crystallochemical control coupled with As–Sb fractionation determines the distribution of silver in many zoned Pb–Zn–Cu–Ag deposits.

Introduction

The sulfosalts of interest here, Fe- and Zn-bearing tetrahedrite-tennantite solid solutions, are common constituents of polymetallic base metal sulfide deposits (e.g., Riley, 1974; Barton et al., 1977; Wu and Petersen, 1977; Einaudi, 1977; Knight, 1977; Loucks, 1984) and bonanza precious metal deposits (Hackbarth et al., 1981; Hackbarth and Petersen, 1983).[1] They are the most common economic ore minerals of silver and often contain at least trace amounts of Hg, Bi, Te, Cd, Pb, and Se. They typically approximate the simple stoichiometry

$$(Cu,Ag)_6^{TRG}[Cu_{2/3}(Fe,Zn,Cd,Hg,Pb)_{1/3}]_6^{TET}(Sb,As,Bi)_4^{SM}(S,Se)_{13}$$

corresponding to an ideal tetrahedrite-tennantite structure with 208 valance electrons per unit cell and full occupancy of the 6 trigonal-planar (TRG), 6 tetrahedral (TET), and 4 semimetal (SM) sites in the 13-sulfur formula unit (e.g., Pauling and Neuman, 1934; Wuensch, 1964, 1966; Springer, 1969; Kalbskopf, 1971, 1972; Hall, 1972; Charlat and Levy, 1974; Pattrick, 1978; Johnson and Jeanloz, 1983; Pattrick and Hall, 1983; Jeanloz and Johnson, 1984; Johnson and Burnham, 1985; Peterson and Miller, 1985). Despite their economic importance, very little is known about the phase relations and thermochemistry of these minerals other than for their synthetic analogues in the simple systems Cu–Sb–S and Cu–Sb–As–S, and Cu–Fe–Sb–S (e.g., Maske and Skinner, 1971; Skinner et al., 1972; Tatsuka

[1] Following Hellner (1958), Nowacki (1969), and Takeuchi and Sadanaga (1969), we use the term sulfosalt to encompass all sulfides in which semimetals are bonded to three sulfurs in a pyramidal arrangement. In the ensuing discussion sulfosalt solid solutions commonly described using the names tetrahedrite, tennantite (or binnite), and freibergite will be referred to as tetrahedrite-tennantite, and, the names tetrahedrite and tennantite will be reserved for tetrahedrite-tennantite with Sb/(As + Sb + Bi) = 1 and As/(As + Sb + Bi) = 1, respectively.

0003–004X/85/1112–1270$02.00

and Morimoto, 1973, 1977a, 1977b; Luce et al., 1977; Makovicky and Skinner, 1978, 1979). Although the synthetic analogues have the same space group symmetry, $I\bar{4}3m$, they typically deviate from the simple stoichiometry of the classical formula, $Cu_{10+x}Fe_{2-x}(As,Sb)_4S_{13}$, requiring the additional component $Cu_{14}(As,Sb)_4S_{13}$ and/or $Cu_{12}(As,Sb)_{14/3}S_{13}$ to describe their composition for positive values of x (Tatsuka and Morimoto, 1977; Makovicky and Skinner, 1978). Measurements of electrical resistivity and optical absorption spectra suggest that tetrahedrite-tennantites with 208 valence electrons per unit cell are large-gap semiconductors, whereas those with between 204 and 208 valence electrons appear to be metallic (Johnson and Jeanloz, 1983; Jeanloz and Johnson, 1984).

Our interest in tetrahedrite-tennantite solid solutions derives, in part, from their potential to serve as sliding scale indicators of the physicochemical environment of ore deposition (e.g., Barton and Skinner, 1979). To date, pyrrhotite and particularly sphalerite are the mineral solutions which have been most widely applied to the study of hydrothermal ore deposits (e.g., Toulmin and Barton, 1964; Barton and Toulmin, 1966; Boorman, 1967; Scott and Barnes, 1971; Barton and Skinner, 1979). As noted by Barton and Skinner (1979, p. 365), "the usefulness of sphalerite derives from its desirable quenching properties, capacity for a wide range of Fe–Zn substitution, widespread occurrence in natural environments, and near ideality for examination by optical and X-ray methods". Among other common ore minerals, tetrahedrite-tennantite is perhaps the most promising as a chemical indicator of hydrothermal mineralizing environments, because it has considerable compositional variability, forms as a primary mineral over a broad range of temperature—e.g., ca. 375°C at Darwin, California (Czamanske and Hall, 1975) to 200°C at Topia, Durango, Mexico (Loucks, 1984)—and is present as at least an accessory mineral in most Pb–Zn–Cu–Ag deposits. Tetrahedrite-tennantite reacts slowly in the laboratory (e.g., Skinner et al., 1972), and preservation of marked compositional discontinuities in natural growth-zoned crystals demonstrates that initial compositions are commonly retained in nature, at least at the lower temperatures of epithermal mineralization, <300°C (e.g., Yui, 1971; Wu and Petersen, 1977; Raabe and Sack, 1984; Hackbarth and Petersen, 1984). Unfortunately, the chemical complexity of tetrahedrite-tennantite has thwarted attempts to acquire the thermodynamic information necessary to interpret the factors influencing its compositional variation.

This paper reports results of Fe–Zn–Cu exchange experiments between sphalerites and tetrahedrite-tennantite in portions of the Cu–Fe–Zn–Sb–S, Cu–Fe–Zn–As–S, and Cu–Fe–Zn–Sb–As–S systems at 500°C. Results of these experiments bear on (1) elucidating the zoning mechanism responsible for the covariance between (As/Sb) and (Fe/Zn) ratios often observed in natural tennahedrites (e.g., Bushnell, 1983; Raabe and Sack, 1984), (2) defining the composition variables of sphalerite and tetrahedrite-tennantite in the low-variance assemblage sphalerite + ISS[2] + arsenopyrite + tetrahedrite-tennantite and (3) defining activity–composition relations for copper-bearing components in sphalerite and ISS (e.g., Hutchison and Scott, 1981). Together with natural tetrahedrite-tennantite-bearing assemblages (e.g., Loucks, 1984; Raabe and Sack, 1984) and preliminary results of similar exchange experiments at 365 and 435°C, they provide a basis for developing a provisional calibration for the thermodynamic mixing properties of $(Ag,Cu)_6(Cu_{2/3}(Fe,Zn)_{1/3})_6(As,Sb)_4S_{13}$ tetrahedrite-tennantite.

Experimental methods

Elements of purity exceeding 99.99% were used as starting materials for the synthesis of (Zn,Fe)S sphalerites and $Cu_{10}(Zn,Fe)_2(Sb,As)_4S_{13}$ tetrahedrite-tennantites. Homogeneous tetrahedrite-tennantites with ratios of Fe/(Fe + Zn) of 0.00, 0.35, 0.60, 0.90 and 1.00, and As/(As + Sb) of 0.00, 0.65, and 1.00 were synthesized from HCl-cleaned 0.5 mm diameter copper wire (m5N-Johnson Matthey Puratonic, Alfa Ventron #400338), 2-mm-diameter iron wire (m4N85-J.M.P., A.V. #00027), antimony ingot (m5N5, A.V. #00032), fire-polished lumps of arsenic (m6N, A.V. #00034), and random pieces of sulfur (t5N5, A.V. #00318). Tetrahedrites, tetrahedrite-tennantite, and tennantites were prepared in 1.5 to 4 gm quantities by initially combining presynthesized FeS with other elements (weighed accurately to $4\frac{1}{2}$ decimal places) and with LiCl–KCl flux in evacuated silica tubes at 400°C in one-atmosphere furnaces for times between 3 weeks and 2 months (Boorman, 1967; Kullerud, 1971). These charges were then annealed at temperatures between 500° (tennantites) and 575°C (tetrahedrites) for times between two and three months. The contents of quenched charges were washed in distilled water to remove flux, dried with acetone, and examined with the optical microscope and electron microprobe. This examination revealed that all tetrahedrites and tetrahedrite-tennantites with Fe/(Fe + Zn) ratios of 0.00, 0.35, and 0.60 were homogeneous with respect to Fe/Zn ratios, whereas the remaining tetrahedrite-tennantites and tennantites were not. Consequently, the tennantites and iron-rich tetrahedrite-tennantites were rerun until homogeneity with respect to (Fe/Zn) ratio could be established from electron microprobe analyses. Repeated attempts at 500°C synthesis of $Cu_{10}Fe_2As_4S_{13}$ were unsuccessful, but Springer (1969, sample 13) reports a lower temperature natural tennantite that closely approaches this composition.

Homogeneous sphalerites with Fe/(Fe + Zn) ratios of 0.005, 0.010, 0.020, 0.050, 0.100, 0.170, and 0.250 were prepared from end-member ZnS sphalerite and FeS troilite by interdiffusion in the presence of NaCl–KCl flux in evacuated silica tubes at 850°C for times between 2 and 4 months. End-member ZnS was prepared by combining H_2-reduced zinc powder with excess sulfur at 500°C for 2 weeks, and then removing excess sulfur by rinsing with carbon disulfide. Stoichiometric FeS was synthesized from H_2-reduced iron powder and sulfur crystals in evacuated silica tubes at 800°C. To ensure FeS stoichiometry, the contents were subsequently resealed with chunks of iron metal; following

[2] ISS is the cubic, Cu–Fe disordered "intermediate solid solution" having the $F\bar{4}3m$ sphalerite structure and a broad composition field in the central part of the Cu–Fe–S system above 200°C (Cabri, 1973). Chalcopyrite is cubic only above 547°C (Yund and Kullerud, 1966).

Table 1. Electron microprobe analyses of run products of Fe-Zn exchange experiments at 500°C. Values in wt.% elements, followed by standard deviation in parentheses. N* = number of point analyses. "Fe/Fe + Zn" refers to starting compositions. Superscript 1 in As and Sb columns designates values of As and Sb not analyzed, but assumed equal to proportions in starting tetrahedrite-tennantite (run products contain only sphalerite and tetrahedrite-tennantite).

EXP#	Phase	Fe/Fe+Zn	S	As	Sb	Fe	Zn	Cu	Sum	N*
2	TD	0.350	24.81(19)		29.00(20)	0.51(03)	7.45(07)	37.21(29)	98.98	(8)
2	SPH	0.005	32.83(22)			0.50(04)	65.55(20)	0.03(03)	98.91	(7)
3	TD	0.600	24.68(22)		29.06(25)	0.74(03)	7.41(17)	37.31(25)	99.20	(8)
3	SPH	0.005	32.78(31)			0.75(04)	65.44(96)	0.01(05)	98.98	(7)
4	TD-TN	0.000	26.70(39)	12.48[1]	10.92[1]	0.38(04)	8.44(30)	39.46(67)	98.38	(8)
4	SPH	0.005	31.61(05)			0.28(01)	65.75(17)	0.04(01)	97.68	(2)
5	TD-TN	0.350	27.22(08)	12.72[1]	11.13[1]	0.97(01)	7.92(07)	39.60(17)	99.56	(2)
5	SPH	0.005	32.90(17)			0.44(03)	65.84(42)	0.05(03)	99.23	(5)
6	TD-TN	0.600	27.20(08)	12.73[1]	11.13[1]	1.28(02)	8.34(04)	39.20(10)	99.91	(4)
6	SPH	0.350	32.48(23)			0.55(02)	65.78(29)	0.05(02)	98.86	(3)
7	TN	0.000	28.11(10)	20.11(21)		0.42(02)	8.70(12)	42.26(12)	99.60	(5)
7	SPH	0.005	32.86(19)			0.22(02)	66.47(32)	0.04(05)	99.59	(3)
8	TN	0.350	28.01(19)	20.16(14)		1.35(03)	7.30(12)	42.37(66)	99.19	(8)
8	SPH	0.005	32.92(27)			0.53(04)	65.93(47)	0.06(09)	99.44	(4)
10	TD	0.000	24.76(16)		29.17(25)	0.44(01)	7.49(09)	37.45(47)	99.30	(9)
10	SPH	0.010	32.97(24)			0.50(03)	65.89(39)	0.06(05)	99.42	(12)
11	TD	0.350	24.95(17)		28.94(23)	0.84(04)	7.37(08)	37.71(45)	99.81	(9)
11	SPH	0.010	32.94(29)			0.91(05)	65.16(76)	0.06(09)	99.07	(9)
12	TD	0.600	24.82(23)		29.09(29)	1.00(02)	7.31(07)	37.57(76)	99.79	(7)
12	SPH	0.010	33.24(22)			0.96(06)	65.34(44)	0.06(04)	99.60	(12)
13	TD-TN	0.000	26.91(12)	12.73(24)	11.16(27)	0.79(02)	7.61(03)	40.15(32)	99.35	(8)
13	SPH	0.010	32.70(21)			0.53(05)	65.77(5)	0.06(03)	99.00	(3)
14	TD-TN	0.350	26.79(39)	12.68(33)	11.11(16)	1.07(03)	7.69(23)	40.56(43)	99.90	(5)
14	SPH	0.010	33.14(24)			0.63(04)	65.89(58)	0.03(03)	99.69	(6)
15	TD-TN	0.600	26.67(12)	12.64(13)	10.79(42)	1.65(01)	6.76(14)	40.34(08)	98.85	(3)
15	SPH	0.010	32.72(14)			0.81(01)	65.04(07)	0.01(01)	98.58	(4)
18	TN	0.350	28.10(16)	20.21(13)		1.75(03)	7.51(34)	42.20(30)	99.77	(4)
18	SPH	0.010	32.35(13)			0.75(01)	65.44(37)	0.09(02)	98.63	(3)
19	TN	0.600	27.94(06)	20.07(19)		2.07(07)	7.34(08)	42.32(15)	99.77	(3)
19	SPH	0.010	32.65(27)			0.89(03)	65.86(16)	0.07(01)	99.47	(4)
21	TD	0.000	24.75(23)		29.07(40)	0.86(02)	7.90(03)	37.49(42)	100.06	(13)
21	SPH	0.020	32.96(22)			1.09(02)	66.12(51)	0.06(05)	100.23	(6)
24	TD	0.900	24.98(12)		29.22(18)	1.40(03)	7.02(31)	37.31(39)	99.94	(14)
24	SPH	0.020	33.15(34)			1.74(02)	65.13(23)	0.09(04)	100.11	(4)
25	TD-TN	0.000	27.46(21)	12.55(21)	11.19(43)	1.48(05)	7.18(14)	40.72(16)	100.58	(7)
25	SPH	0.020	33.14(24)			0.63(04)	65.89(58)	0.03(03)	99.69	(6)
26	TD-TN	0.350	27.25(32)	12.72(16)	11.16(52)	1.80(03)	6.78(24)	40.42(20)	100.13	(5)
26	SPH	0.020	32.70(31)			1.23(03)	65.27(24)	0.05(04)	99.27	(4)
27	TD-TN	0.600	27.27(85)	12.72(27)	11.22(10)	2.05(05)	6.91(38)	40.27(45)	100.44	(8)
27	SPH	0.020	32.60(28)			1.35(02)	65.15(45)	0.06(04)	99.16	(7)
28	TD-TN	0.900	27.39(37)	12.85(38)	11.30(42)	2.38(05)	6.66(28)	41.28(32)	101.86	(10)
28	SPH	0.020	32.62(74)			1.59(21)	65.41(48)	0.06(01)	99.68	(5)
31	TN	0.600	28.57(27)	20.28(14)		2.53(03)	6.65(40)	42.71(22)	100.42	(5)
31	SPH	0.020	32.73(34)			1.26(07)	65.40(20)	0.09(03)	99.53	(8)
32	TN	0.900	28.21(21)	20.33(23)		3.06(10)	6.65(61)	42.77(28)	101.02	(15)
32	SPH	0.020	32.98(34)			1.64(05)	66.44(76)	0.09(05)	101.26	(14)
33	TD	0.000	24.81(17)		29.09(23)	1.81(07)	6.67(24)	37.34(55)	99.73	(11)
33	SPH	0.050	33.09(52)			2.67(23)	64.18(137)	0.10(09)	100.02	(20)
34	TD	0.350	24.82(42)		28.72(28)	2.05(03)	6.87(13)	37.00(56)	99.46	(5)
34	SPH	0.050	32.23(19)			2.87(02)	62.84(22)	0.06903)	99.00	(4)
37	TD-TN	0.000	27.20(52)	12.70(13)	11.14(38)	2.65(05)	6.00(22)	40.50(48)	100.19	(8)
37	SPH	0.050	32.83(39)			2.38(12)	64.55(69)	0.12(04)	99.89	(6)
38	TD-TN	0.350	27.22(59)	12.46(16)	11.17(22)	3.02(04)	6.01(17)	40.51(16)	100.39	(11)
38	SPH	0.050	33.05(41)			2.68(03)	63.64(47)	0.11(05)	99.48	(6)
40	TD-TN	0.900	27.81(38)	12.70(38)	11.24(40)	3.59(04)	5.12(14)	40.47(49)	100.93	(7)
40	SPH	0.050	32.79(83)			3.15(03)	62.72(22)	0.12(05)	98.78	(3)
41	TN	0.000	28.56(22)	20.21(19)		2.93(13)	6.63(10)	42.70(56)	101.33	(10)
41	SPH	0.050	33.44(15)			2.54(11)	64.28(53)	0.20(06)	101.46	(11)
42	TN	0.350	28.78(40)	20.30(41)		3.82(05)	5.15(36)	42.85(79)	100.90	(9)
42	SPH	0.050	33.54(17)			2.76(05)	63.85(44)	0.15(02)	100.29	(10)
43	TN	0.600	28.65(15)	20.43(16)		3.99(02)	5.22(06)	42.98(71)	101.26	(6)
43	SPH	0.050	33.68(22)			2.91(05)	64.28(62)	0.13(07)	101.19	(11)
45	TD	0.000	24.90(11)		29.41(28)	2.92(05)	5.61(22)	37.69(45)	100.45	(10)
45	SPH	0.100	33.27(19)			4.95(06)	61.21(34)	0.11(03)	99.54	(4)
45	ISS		35.28(43)		0.06(05)	33.17(15)	4.23(60)	28.83(31)	101.56	(3)
46	TD	0.350	24.94(18)		29.47(14)	3.09(07)	5.29(39)	37.33(46)	100.11	(8)
46	SPH	0.100	33.39(20)			5.37(08)	61.10(43)	0.07(04)	99.94	(10)
46	ISS		34.75(30)		0.10(08)	33.77(32)	3.59(26)	27.93(26)	100.14	(4)
47	TD	0.600	24.98(16)		29.33(23)	3.23(02)	5.19(19)	37.54(36)	100.27	(6)
47	SPH	0.100	33.23(19)			5.75(10)	60.20(44)	0.16(04)	99.34	(5)
48	SPH	0.100	33.98			5.88	61.29	0.43	101.58	(1)
48	ISS		35.63		0.79	35.48	3.22	27.22	102.33	(1)
49	TD-TN	0.000	27.56(21)	12.95(59)	10.94(19)	4.14(06)	4.42(08)	39.60(53)	99.61	(6)
49	SPH	0.100	32.58(09)			5.16(17)	61.52(56)	0.17(04)	99.43	(4)
51	TD-TN	0.600	26.81(32)	12.40(35)	10.91(18)	4.56(05)	4.54(36)	40.50(11)	99.72	(5)
51	SPH	0.100	32.92(30)			5.56(15)	60.82(47)	0.16(03)	99.47	(10)
52	TD-TN	0.900	27.47(16)	12.74(42)	11.57(46)	4.74(05)	4.57(11)	40.51(23)	101.60	(10)
52	SPH	0.100	33.24(42)			5.73(06)	61.24(42)	0.17(04)	100.33	(7)
53	TN	0.000	28.45(23)	20.53(41)		4.97(10)	4.41(33)	42.58(58)	100.93	(20)
53	SPH	0.100	33.35(24)			4.66(16)	61.96(15)	0.21(04)	100.18	(4)
54	SPH	0.100	34.07			5.18	60.91	0.54	100.70	(1)
54	ISS		35.00			33.33	2.91	29.22	100.46	(1)
55	TN	0.600	28.76(30)	20.38(26)		5.39(12)	3.64(09)	42.94(57)	100.65	(11)
55	SPH	0.100	33.36(28)			5.59(08)	60.97(47)	0.29(13)	100.21	(9)
55	ISS		34.66(17)	2.49(-)		30.96(12)	3.25(27)	28.12(1.16)	99.48	(2)
56	TN	0.900	28.46(37)	20.31(26)		5.29(05)	3.80(38)	41.98(19)	99.80	(4)
56	SPH	0.100	33.51(27)			5.70(08)	61.09(27)	0.27(09)	100.57	(12)
56	ISS		34.79(30)	1.76(07)		32.74(14)	3.19(10)	27.68(15)	100.16	(3)
57	TD	0.350	25.21(24)		29.62(27)	4.47(13)	4.94(33)	36.02(64)	100.26	(13)
57	SPH	0.170	33.50(36)			9.21(03)	57.24(56)	0.10(03)	100.05	(3)
57	ISS		34.95(25)		0.14(01)	36.31(16)	3.62(07)	24.63(09)	99.64	(5)
58	TD	0.600	25.33(20)		29.53(13)	4.58(05)	4.60(09)	36.57(24)	100.61	(8)
58	SPH	0.170	33.30(34)			9.95(10)	56.26(13)	0.21(04)	99.72	(4)
59	TD	0.900	25.10(15)		29.68(18)	4.61(03)	4.60(07)	36.63(05)	100.62	(5)
59	SPH	0.170	33.21(28)			9.57(11)	56.05(53)	0.30(05)	99.13	(8)
59	ISS		34.71(22)		0.10(03)	37.46(17)	2.77(14)	24.40(31)	99.44	(3)
60	TD	1.000	24.95(31)		29.27(15)	4.73(08)	4.67(22)	35.93(37)	99.57	(9)
60	SPH	0.170	33.20(27)			9.90(14)	55.63(27)	0.19(01)	98.92	(6)
61	TD-TN	0.350	27.78(25)	12.57(12)	11.19(24)	5.74(09)	3.94(21)	39.25(45)	100.47	(5)
62	TD-TN	0.600	27.67(17)	12.57(21)	10.89(34)	5.75(07)	3.69(08)	39.38(18)	99.95	(6)
62	SPH	0.170	33.27(39)			9.31(28)	56.75(42)	0.22(03)	99.47	(13)
63	TD-TN	0.900	27.42(33)	12.51(13)	11.67(34)	5.92(10)	3.64(21)	39.19(32)	100.35	(7)
63	SPH	0.170	33.38(50)			9.58(22)	56.67(76)	0.23(06)	99.82	(12)
64	TD-TN	1.000	28.06(40)	12.83(55)	11.11(56)	5.88(11)	3.39(13)	39.74(26)	101.01	(10)
64	SPH	0.170	33.05(30)			9.87(29)	56.38(29)	0.19(03)	99.44	(12)
65	TN	0.350	28.61(15)	20.62(12)		6.30(05)	2.96(12)	42.72(42)	101.22	(11)
65	SPH	0.170	33.46(26)			9.18(15)	57.23(99)	0.34(08)	100.21	(10)
65	ISS		33.15(13)	0.82(-)		36.29(21)	3.64(09)	24.74(14)	100.65	(3)
66	TN	0.600	29.14(24)	20.72(21)		6.38(08)	2.91(11)	42.44(31)	101.58	(8)
66	SPH	0.170	33.76(35)			9.50(19)	57.41(50)	0.32(06)	101.03	(12)
66	ISS		34.66(13)	2.09(04)		34.24(16)	3.44(08)	25.40(24)	99.84	(3)
67	TN	0.900	28.53(7)	20.89(14)		6.43(13)	3.38(19)	42.01(40)	100.74	(7)
67	SPH	0.170	33.61(34)			9.22(22)	57.98(44)	0.31(06)	101.02	(11)
67	ISS		35.35(21)	1.14(12)		35.27(13)	3.62(17)	24.99(08)	100.38	(3)
69	ISS		35.02(14)		0.15(01)	38.84(12)	4.43(07)	21.47(21)	99.91	(3)
70	TD	0.900	24.99(19)		29.86(28)	5.69(09)	3.92(19)	35.41(47)	99.84	(17)
70	SPH	0.250	33.57(27)			14.23(07)	51.04(43)	0.35(04)	99.19	(5)
71	TD	1.000	25.23(12)		29.46(20)	5.51(03)	3.94(13)	35.22(26)	99.37	(9)
71	SPH	0.250	33.87(30)			13.81(25)	52.50(48)	0.33(02)	100.51	(7)
71	ISS		34.89(07)		0.14(01)	38.60(11)	3.88(12)	21.09(09)	98.60	(3)
72	TD-TN	0.600	26.85(68)	8.97(46)	16.71(97)	5.98(10)	3.67(18)	38.04(47)	100.22	(6)
72	SPH	0.250	32.68(32)			10.20(09)	55.25(15)	0.21(04)	98.27	(3)
72	ISS		34.29(20)	0.48(10)		36.21(05)	3.99(04)	23.36(09)	98.33	(2)
72	ASP		21.30(34)	44.04(18)		33.78(02)	1.95(02)	0.07(04)	101.14	(3)
72	ASP		21.48(08)	42.32(24)		34.39(17)	2.15(02)	0.06(03)	101.40	(3)
77	TN	0.900	28.95(21)	20.78(20)		6.63(10)	2.93(13)	42.50(56)	101.79	(8)
77	ISS		34.75(08)	1.88(04)		34.68(12)	3.30(11)	24.77(28)	99.38	(3)
77	ASP		20.43(52)	46.56(69)		34.63(17)	1.43(07)	0.21(03)	103.26	(3)

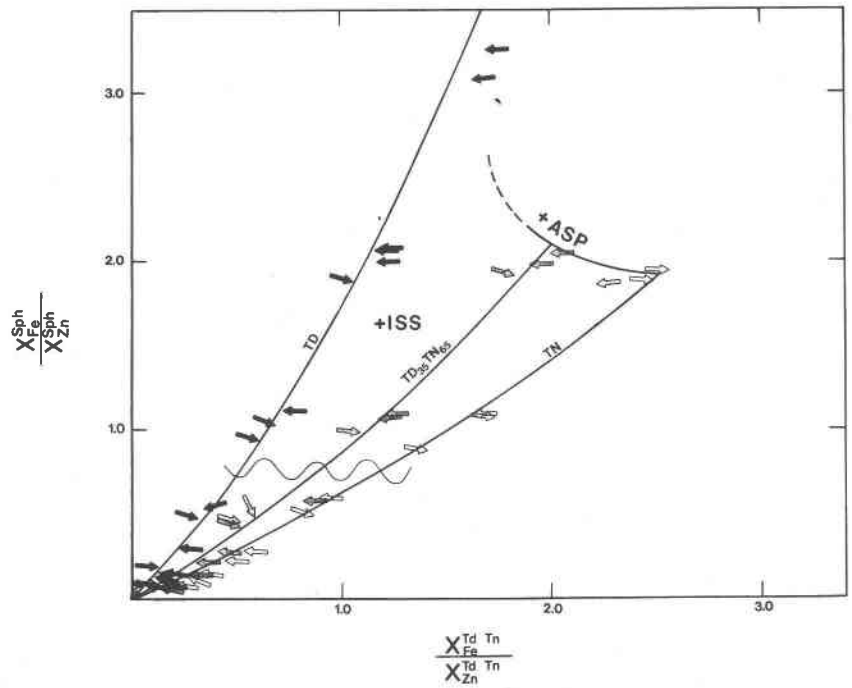

Fig. 1. Fe–Zn exchange isotherms for tetrahedrite-sphalerite, tetrahedrite-tennantite-sphalerite, and tennantite-sphalerite assemblages at 500°C. The vertical and horizontal axes represent the molar ratios of iron to zinc in sphalerite and sulfosalt. Arrows indicate the direction of change of Fe/Zn ratios of sphalerite and tetrahedrite-tennantite during the exchange experiments. Tips of solid, shaded, and open arrows represent sphalerite + tetrahedrite, sphalerite + tetrahedrite-tennantite, and sphalerite + tennantite assemblages, respectively. Wavy line indicates approximate sphalerite compositions required to form ISS by reactions (1) and (2). Curve with dashed extension represents the limit of the ISS + tetrahedrite-tennantite + sphalerite assemblage due to reactions to form arsenopyrite. Solid lines represent calculated isotherms (see caption to Fig. 4).

quenching these chunks were removed from the disaggregated troilite with a magnet.

Seventy-seven combinations of synthetic sphalerites and tetrahedrite-tennantite were selected to provide reversal brackets on the Fe–Zn exchange isotherm at 500°C (see Table 1). Due to the known refractory properties of sphalerite (e.g., Barton and Toulmin, 1966), it was decided to "make tetrahedrite-tennantite do the work" in attaining Fe-Zn exchange equilibrium, so in each experiment sphalerite and tetrahedrite–tennantite were run in the mass proportions 0.04 g sphalerite : 0.005 g tetrahedrite. This ratio corresponds to atomic proportions of about 60 : 1 in terms of exchangable Fe + Zn. These mixtures were combined with LiCl–KCl flux, sealed in silica tubes under vacuum, and heated in one atmosphere furnaces for slightly over 5 months at 500°C, 10 months at 365°C, and 14 months at 435°C. During this period the furnace temperatures were monitored regularly for controller drift using reference chromel-alumel thermocouples calibrated against the melting points of Se (217°C), Te (450°C) and Sb (631°C). These temperature measurements demonstrate that the temperatures of the charges were controlled within $\pm 3°$ during the experiments.

The quenched products of the exchange experiments were washed free of flux and mounted in cold-setting epoxy, polished, and examined by reflected light microscopy and electron microprobe analysis. Electron microprobe analyses of the products of the exchange experiments were accomplished utilizing the eight-spectrometer ARL-SEMQ microprobe interfaced with a PDP-11/10 computer in the Department of Geology and Geophysics of the University of California, Berkeley; microprobe analyses of the starting materials for these experiments were accomplished with the 3-spectrometer ARL-EMX microprobe formerly in the Hoffman Laboratory of Harvard University. In operating both microprobes, operating voltages of 20 kV and sample currents near 0.03 μA (on MgO) were employed, and synthetic sphalerites and tetrahedrite-tennantite of the compositions $Zn_{0.985}Fe_{0.015}S$, $Zn_{0.600}Fe_{0.400}S$, $Cu_{10}Zn_2Sb_4S_{13}$, $Cu_{10}Fe_2Sb_4S_{13}$, and $Cu_{10}Fe_{0.7}Zn_{1.3}As_4S_{13}$ were used as standards for sphalerites and tetrahedrite-tennantite, respectively. MAGIC IV corrections (Colby, 1972) were used to reduce the data. Based on intercomparison of standards, it is believed that the analytical uncertainties are well within the errors generally reported for microprobe analyses, less than $\pm 2\%$ relative for elements present in concentrations greater than 5 wt.%, and less than $\pm 5\%$ for elements present in concentrations between 1 and 5 wt.%. Microprobe analyses demonstrate that the chlorine content of experimental sphalerites and tetrahedrite-tennantites was undetectable in all cases (<0.004 wt.%).

Experimental results

Tetrahedrite-tennantite and sphalerite were observed in the products of all experiments at 500°C. In addition to tetrahedrite-tennantite and sphalerite, the phases ISS and arsenopyrite were observed in some runs. ISS was observed in all charges which had sphalerites with initial X_{FeS}^{SPH} of 0.10, 0.17, and 0.25. In these charges there is a direct correlation between initial X_{FeS}^{SPH} and modal ISS produced. ISS produced in the experiments occurs both as equant grains and as an emulsion of fine specks and lamellae in original

Table 2. Electron microprobe analyses of preliminary experiments that provide the tightest brackets on the Fe-Zn exchange isotherms between sphalerite and tetrahedrite or tennantite at 435 and 365°C. Format as in Table 1.

EXP#	Phase	Fe/(Fe+Zn)	S	As	Sb	Fe	Zn	Cu	Sum	N*
435-35	TD	0.600	25.25(22)		29.30(13)	5.57(08)	2.72(04)	37.85(07)	100.69	(3)
"	SPH	0.050	33.46(05)			2.97(03)	64.05(18)	0.09(02)	100.57	(5)
435-42	TN	0.350	28.05(20)	20.17(12)		4.35(03)	4.69(05)	42.03(18)	99.29	(4)
"	SPH	0.050	32.90(17)			2.87(06)	63.23(60)	0.09(05)	99.10	(4)
435-45	TD	0.000	24.84(23)		29.18(19)	5.77(10)	3.32(02)	37.53(16)	100.64	(4)
"	SPH	0.100	33.30(23)			5.39(13)	60.69(71)	0.07(03)	99.45	(3)
435-48	TD	0.900	25.07(34)		29.21(50)	4.12(07)	4.87(24)	37.34(29)	100.61	(6)
"	SPH	0.100	32.75(22)			6.30(13)	61.60(60)	0.08(03)	100.73	(7)
435-55	TN	0.600	28.25(28)	20.44(19)		5.88(07)	3.75(31)	42.12(36)	100.43	(5)
"	SPH	0.100	33.32(26)			5.64(15)	61.60(36)	0.21(11)	100.77	(5)
435-56	TN	0.900	28.04910)	20.37(31)		6.39(06)	3.21(05)	41.62(43)	99.64	(5)
"	SPH	0.100	32.43(02)			5.97(07)	59.88(20)	0.10(02)	98.38	(2)
435-57	TD	0.350	25.32(14)		29.49(16)	4.74(16)	4.82(32)	36.30(08)	100.66	(4)
"	SPH	0.170	33.67( )			6.69( )	56.15( )	0.31(25)	99.82	(9)
435-69	TD	0.600	25.51(15)		29.58(22)	5.59)07)	3.77(13)	36.22(25)	100.67	(8)
"	SPH	0.250	33.37( )			14.19(08)	51.19(40)	0.25(08)	99.00	(8)
365-71	TD	1.000	24.94(19)		29.50(12)	6.02(03)	2.90(11)	37.40(17)	100.76	(3)
"	SPH	0.250	33.47(33)			14.52(19)	51.16(37)	0.09(03)	99.24	(8)

sphalerite grains. Arsenopyrite was observed only in (1) tennantite-bearing charges with initial X_{FeS}^{SPH} of 0.17 and 0.25, and (2) tetrahedrite-tennantite-bearing charges with the initial X_{FeS}^{SPH} of 0.25. In tetrahedrite-tennantite- and tennantite-bearing charges with X_{FeS}^{SPH} of 0.25, the original sphalerite grains are so pervasively infected with the ISS analogue of "chalcopyrite disease" (e.g., Barton, 1978; Hutchison and Scott, 1981) that it was not possible to obtain adequate electron microprobe analyses of relict sphalerite in these grains. Assuming chemical equilibrium, secondary sphalerites that grew during the experiments suggest approximate values of the composition of sphalerite in the four-phase assemblage in charges with initial X_{FeS}^{SPH} of 0.25 and As/(As + Sb) of 0.65.

Results of electron microprobe analyses of the products of the 500°C Fe–Zn exchange experiments are given in Table 1. The main feature of the electron microprobe analyses is that they demonstrate that the experiments provide tight reversal brackets on the 500°C isotherms for Fe–Zn exchange between sphalerites and tetrahedrites, tetrahedrite-tennantite and tennantites (Fig. 1). These data demonstrate that, at a given Fe/Zn ratio in sphalerite, there is a direct correlation between the Fe/Zn and As/Sb ratios in tetrahedrite-tennantites. In contrast, experiments at 435 and 365°C did not produce similar tight reversal brackets on the Fe–Zn exchange isotherms at these temperatures. Accordingly, only preliminary results for experiments in which tetrahedrite-tennantites exhibit significant changes in Fe/Zn ratios (Fe-rich charges) are reported here (Table 2). Inspection of Figure 1 also reveals that these experiments provide brackets on the Fe/Zn ratios of sphalerites and tetrahedrite-tennantites in the assemblage tetrahedrite-tennantite + sphalerite + arsenopyrite + ISS. X_{FeS}^{SPH} in this four-phase assemblage is 0.159 ± 0.003 for tennantite-bearing charges; for tetrahedrite-tennantite with an As/(As + Sb) ratio of 0.65, X_{FeS}^{SPH} in the five-phase assemblage is bracketed between 0.170 and 0.181 by experiments with initial sphalerites with X_{FeS}^{SPH} of 0.17 and 0.25.

Although the experiments constrain the Fe-Zn exchange isotherms, they do not do so for tetrahedrite-tennantites which have the ideal formula of the initial tetrahedrite-tennantites, $Cu_{10}(Fe,Zn)_2(Sb,As)_4S_{13}$, because they have exchanged Cu with sphalerites initially on the Cu-free join ZnS–FeS. The 52 microprobe analyses listed in Table 1 demonstrate that the Fe–Zn-exchanged tetrahedrite-tennantites have molar (As + Sb)/S ratios well within analytical uncertainty of the 4/13 ratio of the ideal formula ([As + Sb]/S = $(3.9975 \pm 0.0452)/13$. However, relative to the starting materials, all Fe–Zn-exchanged tetrahedrite-tennantites are enriched in (Fe + Zn) and depleted in Cu due to Fe–Cu and Zn–Cu exchange with sphalerites initially on the join FeS–ZnS, and due to the reaction of tetrahedrite-tennantite and sphalerite to form ISS in iron-rich charges. The average composition of all tetrahedrite-tennantites calculated on a 4 semimetal basis (with standard deviations in parentheses), is

$$Cu_{9.720(0.211)}(Fe,Zn)_{2.273(0.167)}(As,Sb)_4S_{13.008(0.148)}$$

which suggests that, to a first approximation, the reactions

$$\underset{\text{TD-TN}}{Cu_{10}Fe_2(As,Sb)_4S_{13}} + \underset{\text{SPH/ISS}}{FeS} = \underset{\text{SPH/ISS}}{CuS} + \underset{\text{TD-TN}}{Cu_9Fe_3(As,Sb)_4S_{13}} \quad (1)$$

and

$$\underset{\text{TD-TN}}{Cu_{10}Zn_2(As,Sb)_4S_{13}} + \underset{\text{SPH/ISS}}{ZnS} = \underset{\text{SPH/ISS}}{CuS} + \underset{\text{TD-TN}}{Cu_9Zn_3(As,Sb)_4S_{13}} \quad (2)$$

adequately describe the removal of Cu to form the Fe–Zn-exchanged tetrahedrite-tennantite. This inference is confirmed by microprobe analyses of ISS, which demonstrate that ISS is on the composition plane CuS–FeS–ZnS, to a close approximation. The average ratio of (Cu + Fe + Zn)/(S + As + Sb) of all ISS's is 0.992 ± 0.028, with Sb being a negligible constituent and As an almost negligible constitutent of ISS.

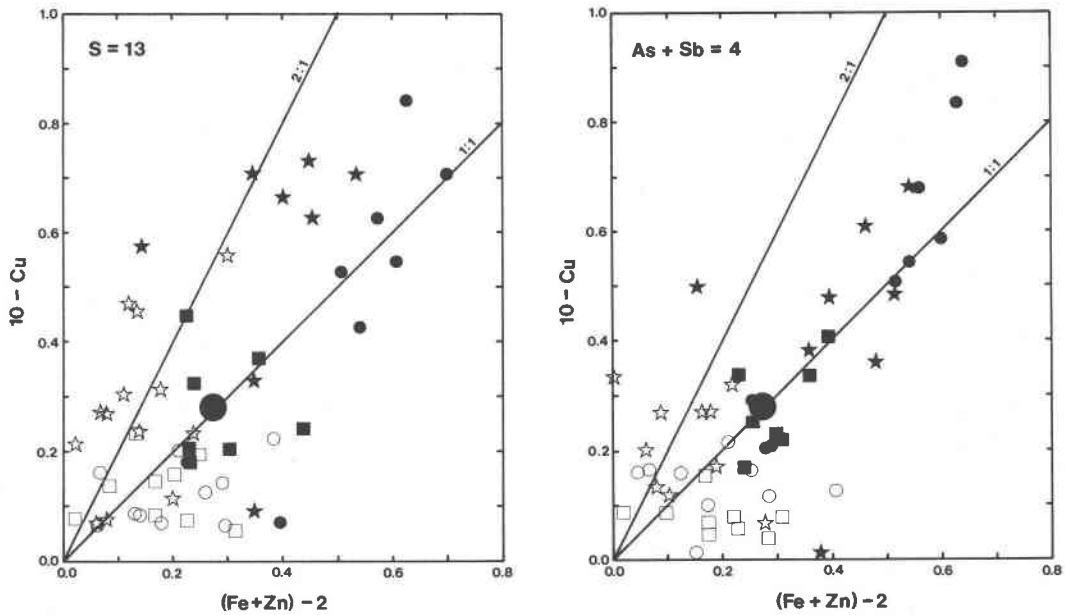

Fig. 2. Deviations of experimental tetrahedrite-tennantites from their initial "ideal" formulas, $Cu_{10}(Fe,Zn)_2(As,Sb)_4S_{13}$, as measured by the quantities (10-Cu) and (Fe + Zn − 2) calculated on the assumption of four semimetals (right figure) and thirteen sulfurs (left figure) per formula unit. Circles, squares, and stars represent tetrahedrites, tetrahedrite-tennantites, and tennantites, respectively. Solid and open symbols differentiate sulfosalts that coexisted with ISS from those that did not, respectively. Large solid circles represent the average of all tetrahedrite-tennantite microprobe analyses calculated on a four semimetal and a thirteen sulfur basis. Lines labeled 2:1 and 1:1 represents the linear arrays which would be defined by tetrahedrite-tennantites displaying the formulas $Cu_{(10-2x)}(Fe,Zn)_{(2+x)}(As,Sb)_4S_{13}$ and $Cu_{(10-x)}(Fe,Zn)_{(2+x)}(As,Sb)_4S_{13}$, respectively.

The progressive removal of Cu from tetrahedrites, tetrahedrite-tennantites, and tennantites with increasing X_{FeS}^{SPH} is illustrated in Figure 2. From Figure 2 it may be noted that although the average tetrahedrite-tennantite plots near the (10 − Cu)/(Fe + Zn − 2) = 1/1 line (i.e., the $[Fe,Zn](Cu)_{-1}$ exchange direction), the data suggest that a line of slightly greater slope relates tetrahedrites, tetrahedrite-tennantite and tennantites in ISS-free and ISS-bearing charges, respectively (i.e., there is a component of the $[(Fe,Zn)](Cu_2)_{-1}$ exchange direction). Although the experimental results do not rule out the operation of the $(Fe,Zn)(Cu_2)_{-1}$ exchange in tetrahedrite-tennantites, they do suggest that at least a large component of the $(Zn,Fe)(Cu)_{-1}$ exchange reaction is required to interrelate Cu-rich and Cu-poor tetrahedrite-tennantites, because available evidence indicates that Zn-rich sphalerites do not depart significantly from ideal (Zn,Fe)S stoichiometry by more than 0.1 atom% (e.g., Kullerud, 1953; Barton and

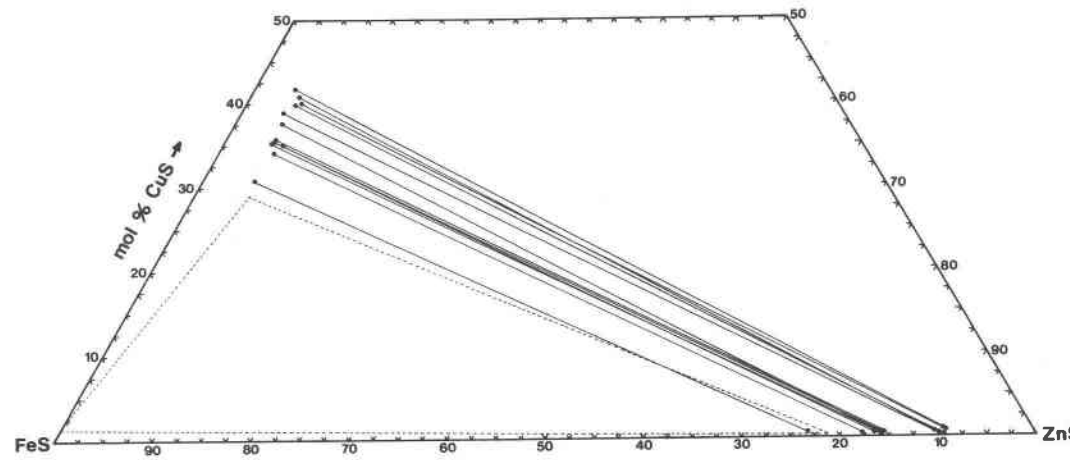

Fig. 3. Projection of ISS–sphalerite phase relations onto the composition plane CuS–FeS–ZnS. Tielines connect coexisting ISS and sphalerite compositions. Vertices of triangle formed by dashed lines represent the compositions of phases in the assemblage ISS–sphalerite–pyrrhotite determined from the calibration of Hutchison and Scott (1981) at 500°C.

Skinner, 1979, p. 366) and ISS is close to the composition plane CuS–ZnS–FeS. Thus, in subsequent discussion, we will assume that our tetrahedrite-tennantites may be described by the formula

$$Cu_{(10-x)}(Fe,Zn)_{(2+x)}(Sb,As)_4S_{13}$$

where x varies between 0 and 0.8 in the Fe–Zn exchanged experimental products.[3] Inspection of Figure 2 reveals that (1) the ordering of tetrahedrites, tetrahedrite-tennantites, and tennantites in terms of x is tetrahedrites > tetrahedrite-tennantites > tennantites at a given X_{FeS}^{SPH}; and (2) x increases progressively with X_{FeS}^{SPH} in ISS-bearing charges.

Unlike tetrahedrite-tennantites, initial and Fe–Zn exchanged sphalerites exhibit minor differences in Cu. Within the analytical uncertainties for elements present in dilute concentrations, values of X_{CuS}^{SPH} in sphalerites saturated with ISS exhibit composition dependence similar to but slightly greater than those given by the calibration of Hutchison and Scott (1981) for sphalerites in the assemblages ISS–sphalerite–pyrite and ISS-sphalerite–pyrite–pyrrhotite (Fig. 3). ISS was the principal sink for Cu removed from tetrahedrite-tennantites in the experiments reported here. The experiments provide tight bounds on ISS–sphalerite tielines in the CuS–FeS–ZnS system for X_{FeS}^{SPH} between 0.086 and 0.245. As shown in Figure 3, these data show that relative to ISS in the assemblages ISS–sphalerite–pyrite and ISS–sphalerite–pyrite–pyrrhotite (e.g., Hutchison and Scott, 1981), ISS on the composition plane CuS–FeS–ZnS in these experiments has a greater Cu/(Cu + Fe + Zn) ratio for the same value of X_{FeS}^{SPH} in coexisting sphalerite.

Interpretation of exchange equilibria in experimental products and natural assemblages

In a first approximation, it is convenient to interpret the experimental data and natural assemblages in terms of a thermodynamic formulation based on the simplified structural formula

$$(Ag,Cu)^{TRG}(Cu_{2/3},(Fe,Zn)_{1/3})_6^{TET}(Sb,As)_4^{SM}S_{13}$$

for tetrahedrite-tennantites in the system Ag–Cu–Fe–Zn–Sb–As–S. As mentioned above, most natural tetrahedrite-tennantite closely correspond to this formula, having negligible departure from full S-site occupancy, only minor amounts of Mn, Cd, Hg, Bi, and Te and, with few exceptions, less than six atoms of Ag per formula unit (e.g., Riley, 1974). It has been established that Ag is highly concentrated in trigonal-planar relative to tetrahedral sites, at least at silver concentrations of several atoms/formula unit (e.g., Kalbskopf, 1971, 1972; Johnson and Burnham, 1985; Peterson and Miller, 1985). Although this site distribution model may not be strictly correct (e.g., Pattrick, 1983), the systematics of the ordering of Ag and Cu between tetrahedral and trigonal-planar sites are not known well enough to justify a less restrictive model. In addition, it should be noted that although metal ratios in some of the experimental tetrahedrite-tennantites deviate substantially from the simplified formula, it will be shown that it is unlikely that these deviations significantly influence Fe–Zn partitioning between tetrahedrite-tennantite and sphalerite.

For the assumptions stated above, the simplest formulation for the thermodynamic properties of tetrahedrite-tennantites requires at least a second degree polynomial in composition variables to describe the vibrational Gibbs energy of tetrahedrite-tennantites, if it is to be consistent with the Fe–Zn exchange data. These data indicate that the As⇌Sb and Fe⇌Zn exchange reactions are coupled energetically; at a given Fe/Zn ratio in sphalerite, an increase in (As/Sb) is accompanied by an increase in Fe/Zn in coexisting tetrahedrite-tennantite. Accordingly, we will provisionally assume that the vibrational Gibbs energy of tetrahedrite-tennantite may be adequately described by a second degree Taylor's series expansion about $Cu_{10}Fe_2Sb_4S_{13}$ (X_1) in terms of the mole fractions of $Cu_{10}Zn_2Sb_4S_{13}$ (X_2), $Cu_{10}Fe_2As_4S_{13}$ (X_3), and $Ag_6Cu_4Fe_2Sb_4S_{13}$ (X_4) components. Such a formulation (e.g., Sack, 1982) leads to the following expression for the vibrational Gibbs energy of tetrahedrite-tennantites:

$$\begin{aligned}\bar{G}^* = {} & \bar{G}^*_{Cu_{10}Fe_2Sb_4S_{13}}(X_1) + \bar{G}^*_{Cu_{10}Zn_2Sb_4S_{13}}(X_2) \\ & + \bar{G}^*_{Cu_{10}Fe_2As_4S_{13}}(X_3) + \bar{G}^*_{Ag_6Cu_4Fe_2Sb_4S_{13}}(X_4) \\ & + \Delta\bar{G}^\circ_{23}(X_2)(X_3) + \Delta\bar{G}^\circ_{24}(X_2)(X_4) + \Delta\bar{G}^\circ_{24}(X_3)(X_4) \\ & + W^{TET}_{FeZn}(X_2)(1-X_2) + W^{SM}_{AsSb}(X_3)(1-X_3) \\ & + W^{TRG}_{AgCu}(X_4)(1-X_4) \qquad (3)\end{aligned}$$

where the $\bar{G}_i^*$'s are the vibrational Gibbs energies of the linearily independent i components,

$$X_2 = 3X_{Zn}^{TET}, \qquad (4)$$

$$X_3 = X_{As}^{SM}, \qquad (5)$$

and

$$X_4 = X_{Ag}^{TRG}, \qquad (6)$$

$\Delta\bar{G}^\circ_{23}$, $\Delta\bar{G}^\circ_{24}$, and $\Delta\bar{G}^\circ_{34}$ are the standard state Gibbs energies of the reciprocal reactions

$$Cu_{10}Zn_2Sb_4S_{13} + Cu_{10}Fe_2As_4S_{13} = Cu_{10}Fe_2Sb_4S_{13} + Cu_{10}Zn_2As_4S_{13}, \qquad (7)$$

[3] In detail, this inference cannot be correct for tetrahedrite-tennantite in arsenopyrite-bearing charges, because arsenopyrite has a S/As ratio considerably less than the 6/4 ratio that would be required to form arsenopyrite by the reaction

$$\underset{\text{TD-TN}}{10Cu_9Fe_3As_4S_{13}} = \underset{\text{TD-TN}}{9Cu_{10}Fe_2As_4S_{13}} + \underset{\text{ASP}}{5FeAs_{0.8}S_{1.2}} + \underset{\text{SPH/ISS}}{7FeS}$$

Therefore at least some of the $(Fe,Zn)(Cu_2)_{-1}$ exchange component is required to interrelate tetrahedrite-tennantites in arsenopyrite-bearing and -free charges due to the reaction

$$\underset{\text{TD-TN}}{2Cu_{10}Fe_2As_4S_{13}} + \underset{\text{SPH/ISS}}{3FeS} = \underset{\text{ASP}}{4FeAsS} + \underset{\text{TD-TN}}{Cu_8Fe_3As_4S_{13}} + \underset{\text{ISS/SPH}}{12CuS}.$$

$$Cu_{10}Zn_2Sb_4S_{13} + Ag_6Cu_4Fe_2Sb_4S_{13} = Cu_{10}Fe_2Sb_4S_{13} + Ag_6Cu_4Zn_2Sb_4S_{13}, \quad (8)$$

and

$$Cu_{10}Fe_2As_4S_{13} + Ag_6Cu_4Fe_2Sb_4S_{13} = Cu_{10}Fe_2Sb_4S_{13} + Ag_6Cu_4Fe_2As_4S_{13}, \quad (9)$$

and W^{TET}_{FeZn}, W^{SM}_{AsSb}, and W^{TRG}_{AgCu} are binary regular-solution-type energy terms which describe deviations from linearity in vibrational Gibbs energy along joins between endmember components differing only in concentrations of Fe and Zn, As and Sb, and Ag and Cu, respectively. An expression for the total Gibbs energy may be obtained by combining (3) with an expression for the configurational entropy of a tetrahedrite-tennantite with the "ideal" stoichiometry

$$\begin{aligned}\bar{S}^{IC} = -R[&2X_2 \ln (X_2/3) + 2(1 - X_2) \ln ((1 - X_2)/3) \\ &+ 4 \ln (2/3) + 4X_3 \ln X_3 + 4(1 - X_3) \ln (1 - X_3) \\ &+ 6X_4 \ln X_4 + 6(1 - X_4) \ln (1 - X_4)] \end{aligned} \quad (10)$$

through the relation

$$\bar{G} = \bar{G}^* - T\bar{S}^{IC}. \quad (11)$$

From this relation for the Gibbs energy, the chemical potential of any endmember component j may be readily obtained by application of the Darken equation (e.g., Darken and Gurry, 1953)

$$\mu_j = \bar{G} + \sum_i n_i(1 - X_i)\left(\frac{\partial \bar{G}}{\partial X_i}\right)_{P,T,X_k/X_l} \quad (12)$$

where the n_i's are the mole fractions of the linearily independent components $Cu_{10}Fe_2Sb_4S_{13}$, $Cu_{10}Zn_2Sb_4S_{13}$, $Cu_{10}Fe_2As_4S_{13}$, and $Ag_6Cu_4Fe_2Sb_4S_{13}$ in tetrahedrite-tennantite component j (e.g., these n_i are $= -2, +1, +1, +1$, respectively, for the component $Ag_6Cu_4Zn_2As_4S_{13}$).

Applications of the Darken equation yield the following expressions for the chemical potentials of the exchange components, the exchange potentials (e.g., Thompson and Thompson, 1976), of principal interest here:

$$\begin{aligned}\mu_{Zn(Fe)_{-1}} &= 1/2(\mu_{Cu_{10}Zn_2Sb_4S_{13}} - \mu_{Cu_{10}Fe_2Sb_4S_{13}}) \\ &= \bar{G}^\circ_{Zn(Fe)_{-1}} + RT \ln [X_2/(1 - X_2)] \\ &\quad + 1/2[\Delta\bar{G}^\circ_{23}(X_3) + \Delta\bar{G}^\circ_{24}(X_4) \\ &\quad + W^{TET}_{FeZn}(1 - 2X_2)], \end{aligned} \quad (13)$$

$$\begin{aligned}\mu_{Ag(Cu)_{-1}} &= 1/6(\mu_{Ag_6Cu_4Fe_2Sb_4S_{13}} - \mu_{Cu_{10}Fe_2Sb_4S_{13}}) \\ &= \bar{G}^\circ_{Ag(Cu)_{-1}} + RT \ln [X_4(1 - X_4)] \\ &\quad + 1/6[\Delta\bar{G}^\circ_{24}(X_2) + \Delta\bar{G}^\circ_{34}(X_3) \\ &\quad + W^{TRG}_{AgCu}(1 - 2X_4)], \end{aligned} \quad (14)$$

and

$$\begin{aligned}\mu_{As(Sb)_{-1}} &= 1/4(\mu_{Cu_{10}Fe_2As_4S_{13}} - \mu_{Cu_{10}Fe_2Sb_4S_{13}}) \\ &= \bar{G}^\circ_{As(Sb)_{-1}} + RT \ln [X_3/(1 - X_3)] \\ &\quad + 1/4[\Delta\bar{G}^\circ_{23}(X_2) + \Delta\bar{G}^\circ_{34}(X_4) \\ &\quad + W^{SM}_{AsSb}(1 - 2X_3)] \end{aligned} \quad (15)$$

where $\bar{G}^\circ_{Zn(Fe)_{-1}}$, $\bar{G}^\circ_{Ag(Cu)_{-1}}$, and $\bar{G}^\circ_{As(Sb)_{-1}}$ are the quantities

$$1/2(\bar{G}^\circ_{Cu_{10}Zn_2Sb_4S_{13}} - \bar{G}^\circ_{Cu_{10}Fe_2Sb_4S_{13}}),$$

$$1/6(\bar{G}^\circ_{Ag_6Cu_4Fe_2Sb_4S_{13}} - \bar{G}^\circ_{Cu_{10}Fe_2Sb_4S_{13}}),$$

and

$$1/4(\bar{G}^\circ_{Cu_{10}Fe_2As_4S_{13}} - \bar{G}^\circ_{Cu_{10}Fe_2Sb_4S_{13}}),$$

respectively.

$Zn(Fe)_{-1}$ exchange equilibrium

The condition of Zn–Fe exchange equilibrium between tetrahedrite-tennantites and sphalerites may be written as

$$\mu^{TD-TN}_{Zn(Fe)_{-1}} = \mu^{SPH}_{Zn(Fe)_{-1}} \quad (16)$$

where the $Zn(Fe)^{-1}$ exchange potential of tetrahedrite-tennantite is defined by expression (13), and that for (Zn,Fe)S sphalerites may be readily calculated from the following expression for the Gibbs energy of sphalerite

$$\begin{aligned}\bar{G}_{(Zn,Fe)S} &= \bar{G}^\circ_{FeS}X^{SPH}_{FeS} + \bar{G}^\circ_{ZnS}(1 - X^{SPH}_{FeS}) \\ &\quad + RT[X^{SPH}_{FeS} \ln X^{SPH}_{FeS} + (1 - X^{SPH}_{FeS}) \ln (1 - X^{SPH}_{FeS}) \\ &\quad + X^{SPH}_{FeS} \ln \gamma^{SPH}_{FeS} + (1 - X^{SPH}_{FeS}) \ln \gamma^{SPH}_{ZnS}] \end{aligned} \quad (17)$$

given values for the activity coefficients γ^{SPH}_{FeS} and γ^{SPH}_{ZnS}. Values for γ^{SPH}_{FeS} and γ^{SPH}_{ZnS} (for FeS and ZnS components referred to the $F\bar{4}3m$ standard state) appropriate for 500°C may be taken directly from Fleet's (1975) Gibbs–Duhem integration of the data of Barton and Toulmin (1966) for 850°C because a^{SPH}_{FeS}–X^{SPH}_{FeS} relations are insensitive to temperature from at least 340 to 850°C, (Barton and Toulmin, 1966; Scott and Barnes, 1971). Accordingly, if the trivial concentration of Cu in sphalerite is ignored, the condition of $Zn(Fe)^{-1}$ exchange equilibrium between tetrahedrite-tennantite and sphalerite may be written as

$$\begin{aligned}RT \ln K_D &\equiv RT \ln \left[\left(\frac{X^{TET}_{Fe}}{X^{TET}_{Zn}}\right)\left(\frac{X^{SPH}_{ZnS}}{X^{SPH}_{FeS}}\right)\right] \\ &= RT \ln \left(\frac{\gamma^{SPH}_{FeS}}{\gamma^{SPH}_{ZnS}}\right) + \Delta\bar{G}^\circ_{Zn(Fe)_{-1}} \\ &\quad + 1/2\Delta\bar{G}^\circ_{23}(X_3) + 1/2\Delta\bar{G}^\circ_{24}(X_4) \\ &\quad + 1/2W^{TET}_{FeZn}(1 - 2X_2) \end{aligned} \quad (18)$$

where

$$\begin{aligned}\Delta\bar{G}^\circ_{Zn(Fe)_{-1}} &= 1/2(\bar{G}^\circ_{Cu_{10}Zn_2Sb_4S_{13}} - \bar{G}^\circ_{Cu_{10}Fe_2Sb_4S_{13}}) \\ &\quad + (\bar{G}^\circ_{FeS} - \bar{G}^\circ_{ZnS}). \end{aligned} \quad (19)$$

An examination of a plot of $RT \ln K_D$ versus X_{FeS}^{SPH} (Fig. 4) suggests that only two of the three energy parameters which apply to Ag-free systems ($X_4 = 0$) are tightly constrained by the experimental data at 500°C. Values of 2.07 $\pm$ 0.07 and 2.59 $\pm$ 0.14 kcal/gfw are obtained for the energy parameters $\Delta\bar{G}^{\circ}_{Zn(Fe)-1}$ and $\Delta\bar{G}^{\circ}_{23}$ from linear regression of (18) for the data sets defining the reversal brackets on $RT \ln K_D$ over the sphalerite composition range $0.04 < X_{FeS}^{SPH} < 0.25$ and the assumption that $W_{FeZn}^{TET} = 0$. As shown in Figure 4, these results describe all the experimental data

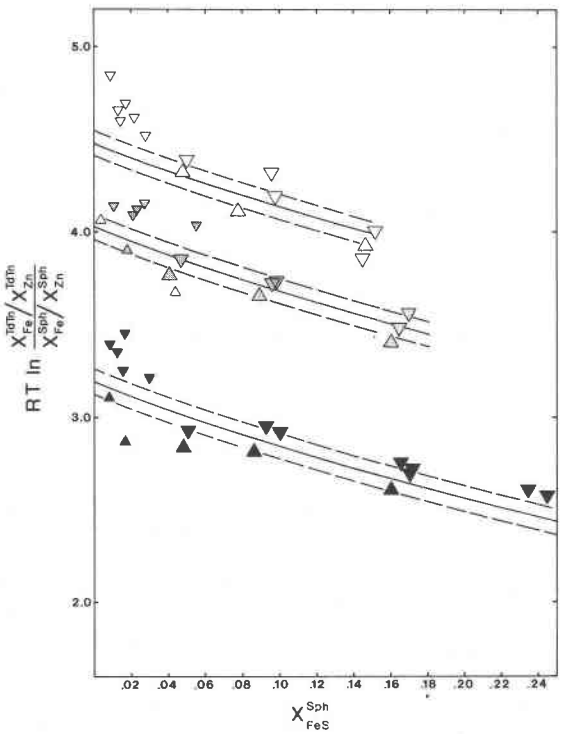

Fig. 4. $RT \ln K_D$ (kcal/gfw) versus mole fraction of FeS in sphalerite at 500°C. Arrows show the direction of change of $RT \ln K_D$ during the exchange experiments; arrow tips represent sphalerite + tetrahedrite (solid), sphalerite + tetrahedrite-tennantite (shaded), and sphalerite + tennantite (black) assemblages. Solid curves represent the calibration of equation (13) for sphalerite + tetrahedrite, sphalerite + tetrahedrite-tennantite, and sphalerite + tennantite assemblages for values of $\Delta\bar{G}^{\circ}_{Zn(Fe)-1}$ and $\Delta\bar{G}^{\circ}_{23}$ of 2.0718 and 2.59 kcal/gfw, and the following expression for $\ln (\gamma_{FeS}^{SPH}/\gamma_{ZnS}^{SPH})$:

$$\ln\left(\frac{\gamma_{FeS}^{SPH}}{\gamma_{ZnS}^{SPH}}\right) = W(X)(1 - 2X_{FeS}^{SPH})$$

where $W(X) = 0.7285 - 0.9186(X_{FeS}) - 0.5295(X_{FeS})^2 - 0.1772(X_{FeS})^3$, and the coefficients of $W(X)$ were determined from the values of $\ln (\gamma_{FeS}^{SPH}/\gamma_{ZnS}^{SPH})$ for $X_{FeS}^{SPH} = 0.1$, 0.2 and 0.3 given in Table 1 of Fleet (1975), and the intercept defined by extrapolating these data to $X_{FeS}^{SPH} = 0$ on a plot of $\ln (\gamma_{FeS}^{SPH}/\gamma_{ZnS}^{SPH})/(1 - 2X_{FeS})$ vs. X_{FeS}^{SPH}. The dashed curves bracketing the solid curves represent the standard error associated with the energy term $\Delta\bar{G}^{\circ}_{Zn(Fe)-1}$ only, $\pm$0.07 kcal/gfw.

to an excellent approximation and are adopted here. Despite the success of the "ideal" reciprocal solution formulation for tetrahedrite-tennantite in treating the Fe–Zn exchange data, we may not conclude, a priori, that tetrahedrite-tennantite behaves ideally with respect to mixing of Fe, Zn, and Cu on tetrahedral sites. Indeed, the experimental data suggest that some consideration of nonideality in the mixing of Cu, Fe, and Zn in tetrahedrite-tennantites is required, as the chords corresponding to constant X_{Sb}^{SM} in Figure 4 appear to exhibit progressive counterclockwise rotation, relative to those for "ideal" tennahedrite, with increasing X_{Sb}^{SM} over the X_{FeS}^{SPH} range of tight reversal brackets on $RT \ln K_D$ for $0.04 < X_{FeS}^{SPH} < 0.17$; the tetrahedrites exhibit the maximum deviation from the ideal formula. These observations suggest that tetrahedrite-tennantites which are enriched in Fe and Zn relative to tetrahedrite-tennantites with the ideal formula have slightly greater values of $RT \ln K_D$ and would thus imply that the values of $\Delta\bar{G}^{\circ}_{Zn(Fe)-1}$ and $\Delta\bar{G}^{\circ}_{23}$ deduced from (18) are minimum and maximum bounds on these energies, respectively. However, we choose not to correct for any deviation from the "ideal" tetrahedrite-tennantite formulation in treating the Fe–Zn exchange data, because any deviations from this formulation are well within the uncertainties of the analytical data and of the determinations of activity–composition relations in sphalerite.

Given the values of $\Delta\bar{G}^{\circ}_{23}$ and $\Delta\bar{G}^{\circ}_{Zn(Fe)-1}$ for 500°C, preliminary reversals on the Fe–Zn exchange isotherms at 435 and 365°C, and composition and temperature data for natural sphalerite + tetrahedrite-tennantite assemblages, it should be relatively straightforward to develop a calibration for the temperature dependence of the distribution coefficient for Fe–Zn exchange between sphalerites and tetrahedrite-tennantites in both silver-free and silver-bearing systems. Unfortunately, there is presently a paucity of composition data on natural sphalerite + tetrahedrite-tennantite assemblages, and the Fe–Zn exchange isotherms at 435 and 365°C are not well constrained by the preliminary results. Thus any calibration developed from such comparisons must be viewed as tentative. Nevertheless, such comparisons do suggest that $\Delta\bar{G}^{\circ}_{23}$ and $\Delta\bar{G}^{\circ}_{Zn(Fe)-1}$ are temperature insensitive over the range 200–500°C. Thus, such comparisons suggest that the Fe–Zn exchange reaction between sphalerite and tetrahedrite-tennantite could be a useful geothermometer for a wide variety of polymetallic base-metal sulfide and bonanza precious-metal deposits, if the compositions of tetrahedrite-tennantites were quenchable over this temperature range.

Approximate constancy of $\Delta\bar{G}^{\circ}_{23}$ and $\Delta\bar{G}^{\circ}_{Zn(Fe)-1}$ over the temperature range 200–500°C may be demonstrated from comparison of the experimental results with composition and temperature data for sphalerite + tetrahedrite-tennantite assemblages from the Hock Hocking mine at Alma, Colorado (Raabe and Sack, 1984) and a gold–quartz vein from Alleghany, California (J. K. Bohlke, pers. comm., 1984). Tetrahedrite-tennantites from both of these localities have negligible concentrations of Ag, and they are close to the "ideal" formula; tetrahedrite-tennantites from the Hock

Hocking mine span virtually the entire range of X_{As}^{SM}. Raabe and Sack (1984) have shown that the covariance of ln (Zn/Fe) and X_{As}^{SM} exhibited by growth-zoned tetrahedrite-tennantites from Hock Hocking mine is consistent with fluid inclusion temperatures from sphalerites ($T = 249 \pm 7$°C) employing the value of $\Delta\bar{G}^{\circ}_{23} = 2.59 \pm 0.14$ kcal/gfw, and the assumption that the Fe/Zn ratio of sphalerite was constant during the growth of tetrahedrite-tennantite. Microprobe analyses do not reveal composition zoning in sphalerites, and they do not exhibit color zoning, a sensitive indicator of composition zoning (e.g., Barton et al., 1963; McLimans et al., 1980). Accordingly, we will adopt the value of $\Delta\bar{G}^{\circ}_{23} = 2.59 \pm 0.14$ kcal/gfw from 200–500°C as the basis for comparison of the experimental Fe-Zn distribution coefficients with natural assemblages, employing for Ag-free tetrahedrite-tennantites equation (18) rewritten in terms of the variables ln K_D and $(1/T)$,

$$\hat{\sigma}_x^* = \ln K_D - \ln \frac{\gamma_{FeS}^{SPH}}{\gamma_{ZnS}^{SPH}} - \frac{\Delta\bar{G}^{\circ}_{23}}{2RT}(X_3)$$

$$= \frac{\Delta\bar{H}^{\circ}_{Zn(Fe)_{-1}}}{R}\left(\frac{1}{T}\right) - \frac{\Delta\bar{S}^{\circ}_{Zn(Fe)_{-1}}}{R} \qquad (20)$$

Such a comparison (Fig. 5) reveals that the simplest assumption, that $\partial\Delta\bar{G}^{\circ}_{23}/\partial T$ and $\partial\bar{G}^{\circ}_{Zn(Fe)_{-1}}/\partial T$ are negligible, is consistent with both the experimental data and natural assemblages, to a first approximation. However, it does not rule out positive values for $\Delta\bar{S}^{\circ}_{Zn(Fe)_{-1}}$, because (1) the values of ln K_D and $\hat{\sigma}_x^*$ defined by the data of Raabe and Sack (1984) are quite uncertain given that $X_{FeS}^{SPH} < 0.003$ and that there is a fair degree of uncertainty in the assumption that $\partial\Delta\bar{G}^{\circ}_{23}/\partial T = 0$, (2) some of the tetrahedrite-tennantites analyzed by Bohlke are in contact with sphalerites with $X_{FeS}^{SPH} \geq 0.02$, and all of them are antimony-rich $[X_{As}^{SM}/(X_{As}^{SM} + X_{Sb}^{SM}) = 0.14 \pm 0.03]$, and (3) the preliminary constraints on the Fe-Zn isotherms at 365 and 435°C will permit counter-clockwise (but not clockwise) rotation of the $\Delta\bar{S}^{\circ}_{Zn(Fe)_{-1}} = 0$ line through the brackets on $\hat{\sigma}_x^*$ at 500°C (in Fig. 5).

Despite the uncertainties associated with the assumptions that $\Delta\bar{G}^{\circ}_{23}$ and $\Delta\bar{G}^{\circ}_{Zn(Fe)_{-1}}$ are constant, it may be readily established that exchange of Ag for Cu in tetrahedrite-tennantites significantly alters the Fe–Zn exchange isotherms from those in Ag-free systems. Ag-bearing tetrahedrites in fissure veins from Topia, Durango, Mexico (Loucks, 1984) ($X_{Ag}^{TRG} = 0.58 \pm 0.08$, $T = 215 \pm 20$°C, $X_{As}^{SM} = 0.022 \pm 0.013$, and $0.06 \leq X_{FeS}^{SPH} \leq 0.13$, for 8 tetrahedrite-tennantite-sphalerite assemblages) have values of $\hat{\sigma}_x^*$ significantly greater than those in Ag-free systems. Comparison of the Topia data with the provisional calibration for the Fe–Zn exchange reaction in Ag-free systems (Fig. 5) suggests that the magnitude of the stabilization of Fe relative to Zn due to the exchange of Ag for Cu is similar to that due to the exchange of As for Sb. Amending (20) to include provision for this stabilization in Ag-bearing tetrahedrite-tennantites,

$$\hat{\sigma}_x^* = \frac{\Delta\bar{G}^{\circ}_{Zn(Fe)_{-1}}}{RT} + \frac{\Delta\bar{G}^{\circ}_{24}}{2RT}(X_4) \qquad (21)$$

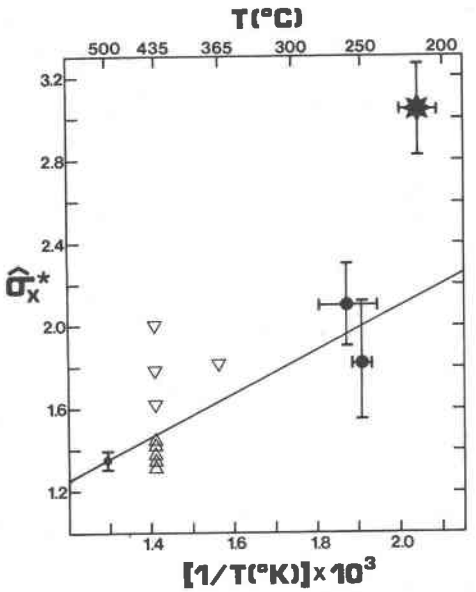

Fig. 5. The variation of $\hat{\sigma}_x^*$ with $(1/T)$ (°K)$^{-1}$. Small circle and associated error bar represent the experimental constraints at 500°C. Arrows indicate preliminary brackets from exchange experiments at 435 and 365°C. Large circles represent the values of $\hat{\sigma}_x^*$ defined by the natural sphalerite + tetrahedrite-tennantite assemblages reported by J. K. Bohlke (pers. comm., 1984; ln $K_D = 2.10 \pm 0.20$, $X_{FeS}^{SPH} = 0.022 \pm 0.004$, and $X_{As}^{SM}/(X_{As}^{SM} + X_{Sb}^{SM}) = 0.14 \pm 0.03$ for three samples) and Raabe and Sack (1984). Fluid inclusion studies establish a temperature of 249 ± 7°C for the tetrahedrite-tennantites assemblages reported by Raabe and Sack (1984). A temperature between 240 and 280°C has been inferred for the sphalerite + tetrahedrite-tennantite assemblages from Allegheny, California. Although most oxygen isotope temperatures of mica-carbonate-quartz assemblages give temperatures between 300 and 340°C for these deposits, fluid inclusion and petrographic studies suggest that the later sulfides were deposited at lower temperatures (J. K. Bohlke, pers. comm., 1984). The star with associated error bar represents the data of Loucks (1984) for tetrahedrites with >18 wt.% Ag. The line crossing Fig. 5 represents the calibration of equation (18) for values of $\Delta\bar{H}^{\circ}_{Zn(Fe)_{-1}}$, $\Delta\bar{H}^{\circ}_{23}$, $\Delta\bar{S}^{\circ}_{Zn(Fe)_{-1}}$, and $\Delta\bar{S}^{\circ}_{23}$ of 2.0718 kcal/gfw, 2.5898 kcal/gfw, 0 Gibbs/gfw, and 0 Gibbs/gfw, and the expression for ln $(\gamma_{FeS}^{SPH}/\gamma_{ZnS}^{SPH})$ given in the caption to Fig. 4.

permits an estimate for $\Delta\bar{G}^{\circ}_{24}$ of 3.0 ± 1.5 kcal/gfw for 215 $\pm$ 20°C and $\Delta\bar{G}^{\circ}_{Zn(Fe)_{-1}} = 2.07 \pm 0.07$ kcal/gfw. This estimate is probably an upper bound on $\Delta\bar{G}^{\circ}_{24}$ for the reasons cited above.

Ag(Cu)$_{-1}$ exchange equilibria

In principle, the variables which express the energetic interdependence of the Ag(Cu)$_{-1}$ and As(Sb)$_{-1}$ exchange reactions and nonideality due to the Ag(Cu)$_{-1}$ exchange, $\Delta\bar{G}^{\circ}_{24}$ and W^{TRG}_{AgCu}, respectively, may be assessed from natural assemblages utilizing the condition of Ag(Cu)$_{-1}$ exchange equilibrium. For this purpose expression (14) for the Ag(Cu)$_{-1}$ exchange potential in tetrahedrite-tennantite may be combined with equivalent statements for $\mu_{Ag(Cu)_{-1}}$

defined by coexisting sulfides or hydrothermal solutions. In practice, however, it is evident that there is presently a paucity of appropriate data, and that it will be necessary to make several assumptions to derive estimates of the parameters $\Delta\bar{G}^{\circ}_{24}$ and W^{TRG}_{AgCu}. Nevertheless, *it is certain* that $\Delta\bar{G}^{\circ}_{34}$ is a large positive number (i.e., $\Delta\bar{G}^{\circ}_{34} \gg \Delta\bar{G}^{\circ}_{23}$ or $\Delta\bar{G}^{\circ}_{24}$) and that the correlations between Ag and Sb commonly observed in tetrahedrite-tennantite suites are largely crystallochemically controlled rather than being simply "permissive" as suggested by Miller and Craig (1983). This conclusion is readily evident from plots of Ag/(Ag + Cu) or Ag versus X^{SM}_{Sb} and could be anticipated from structural refinements of tetrahedrite-tennantites (e.g., Wuench, 1964; Wuench et al., 1966; Kalbskopf, 1972; Johnson and Burnham, 1985; Peterson and Miller, 1985). Examination of Pb-Zn-Cu-Ag sulfide deposits reveals that tetrahedrite-tennantites often exhibit composition zoning in both time and space. Both Sb and Ag tend to be concentrated in earlier growth zones of individual crystals and at the distal ends of paths of fluid flow (e.g., Goodell and Petersen, 1974; Wu and Petersen, 1977; Hackbarth and Petersen, 1984). In addition, correlations between Ag and Sb in tetrahedrite-tennantites along paths of fluid flow typically deviate from linearity on plots of Ag or Ag/(Ag + Cu) versus X^{SM}_{Sb} in a manner which would be predicted from (14) for the assumption of constant $Ag(Cu)_{-1}$ exchange potential and values of $\Delta\bar{G}^{\circ}_{34} \gg \Delta\bar{G}^{\circ}_{23}$ or $\Delta\bar{G}^{\circ}_{24}$.

Despite the paucity of appropriate phase equilibrium constraints, provisional values of $\Delta\bar{G}^{\circ}_{34}$ may be obtained from analysis of trends in $RT \ln (X^{TRG}_{Cu}/X^{TRG}_{Ag})$ versus X^{SM}_{As} of the growth zoned tetrahedrite-tennantite crystals reported by Shimazaki (1974) and those from Julcani, Peru (Kane and Peterson, 1985). If values of $RT \ln (X^{TRG}_{Cu}/X^{TRG}_{Ag})$ are corrected to those which would correspond to a constant value of the $Zn(Fe)_{-1}$ exchange potential in each sample, trends in $RT \ln (X^{TRG}_{Cu}/X^{TRG}_{Ag})$ versus X^{SM}_{As} of tetrahedrite-tennantites are remarkably parallel, except for several samples from Julcani (Fig. 6). It is apparent that most of these trends are strikingly parallel with the covariance trend given by (14) for constant values of the $Zn(Fe)_{-1}$ and $Ag(Cu)_{-1}$ exchange potentials and the assumptions that

$$\Delta\bar{G}^{\circ}_{34} = 3(\Delta\bar{G}^{\circ}_{23} + \Delta\bar{G}^{\circ}_{24}) \qquad (22)$$

(i.e., $\Delta\bar{G}^{\circ}_{34} = 16.8 \pm 4.5$ kcal/gfw) and $W^{TRG}_{AgCu} = 0$.[4] Parallelism of the trends of the tetrahedrite-tennantites of the Kosaka and Shakanai Kuroko deposits is not surprising because they contain the low-variance assemblage pyrite + chalcopyrite + sphalerite + electrum (e.g., Eldridge et al., 1983), an assemblage which defines (but does not buffer) the $Ag(Cu)_{-1}$ exchange potential. Although the striking parallelism of $RT \ln (X^{TRG}_{Cu}/X^{TRG}_{Ag})$ versus X^{SM}_{As} covariation curves and their linearity suggests that $W^{TRG}_{AgCu} \sim 0$ to a first approximation, this conclusion cannot be advanced with certainty because this assemblage does not guarantee that the $Ag(Cu)_{-1}$ exchange potential was fixed to a single value during hydrothermal mineralization. Certainly W^{TRG}_{AgCu} is considerably less than 10.1 kcal/gfw, the upper bound deduced from the consideration that X_4 can assume all values between zero and unity down to temperatures of at least 150°C. Although the Julcani assemblages have higher

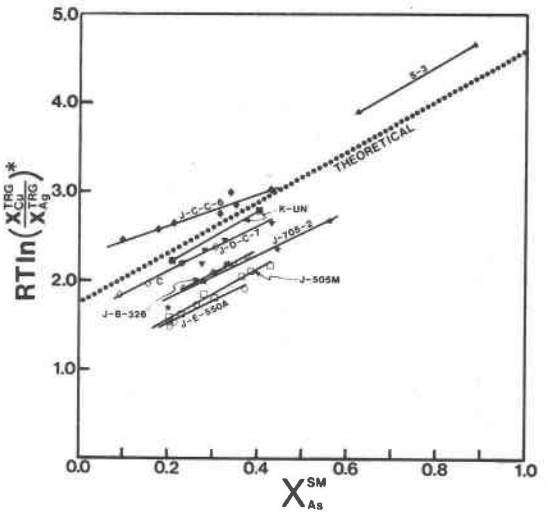

Fig. 6. Variation of the ratio of trigonally coordinated copper/silver with arsenic content in semi-metal sites based on a suite of electron microprobe analyses of natural tetrahedrite-tennantites in samples from Kuroko massive sulfide and vein-type ore deposits. Scatter within individual composition arrays due to the energetic consequences of variation in Zn/Fe (by up to a factor of two) has been removed by recalculating the measured Cu/Ag to the values it would have if $\mu_{Zn(Fe)_{-1}}$ remained constant at its minimum value in the particular sample; i.e.,

$$RT \ln (X^{TRG}_{Cu}/X^{TRG}_{Ag})^{*} = RT \ln (X^{TRG}_{Cu}/X^{TRG}_{Ag}) - (\Delta\bar{G}^{\circ}_{24}/6)[3(X^{TET}_{Zn} - X^{TET}_{Zn(min)})],$$

in kilocalories (cf. equation 14). Slopes of these linear arrays may be compared with the theoretical slope of 2.8 kcal (= 16.8/6) predicted from equation 22. Data sources for Kuroko samples (low-variance assemblages) are as follows: K-UN, Kosaka mine, Uchinotai-Nishi orebody; and S-3, Shakanai mine, number 3 orebody, both from Shimazaki (1974). Data for vein-type samples (high-variance assemblages) are as follows: C, Chitose epithermal silver–gold vein, Hokkaido (Yui, 1971); all samples having a J prefix are from Cu–Pb–Zn–Ag veins in the Mimosa vein system, Julcani, Peru. Temperatures employed in the calculations are 300°C for Kosaka and Shakanai (Pisutha-Arnond and Ohmoto, 1983; Eldridge, Barton, and Ohmoto, 1983); 300°C for Julcani (Petersen et al., 1977, p. 945); and 250°C for Chitose as a "ball-park" estimate typical of this class of deposit. From the large data set available for bismuthian tetrahedrite-tennantite from Julcani, those samples chosen for illustration were selected for low Bi (< 1 wt.%; usually < 0.5 wt.%), relatively large range of As/Sb, and a modest or small range of variation in Zn/Fe. All analyses for these samples are plotted.

[4] This result is equivalent to the assumption that $g_{34} = g_{23} + g_{24}$ in a second degree Taylor's series expansion for the vibrational Gibbs energy in terms of composition variables $X^{TET}_{Zn} = X_2$, $X^{SM}_{As} = X_3$, and $X^{TRG}_{Ag} = X_4$

$$G^{*} = g_0 + g_2(X_2) + g_3(X_3) + g_4(X_4) + g_{23}(X_2)(X_3) + g_{24}(X_2)(X_4) + g_{23}(X_3)(X_4) + g_{22}(X_2)^2 + g_{33}(X_3)^2 + g_{44}(X_4)^2$$

variance in the phase rule sense, the accord between actual and theoretical slopes is nevertheless striking. Therefore, we consider the above to be compelling evidence for strong influence of crystal energetics on Ag content in these tetrahedrite-tennantite-bearing suites, and tentatively adopt a value of 16.8 ± 4.5 kcal for $\Delta\bar{G}^{\circ}_{34}$.

As(Sb)$_{-1}$ exchange equilibria

Very little may be inferred about As(Sb)$_{-1}$ exchange reactions between tetrahedrite-tennantites and other As- and Sb-bearing phases based on presently available experimental and petrological data. Perhaps the only inferences that are secure are (1) that $W^{SM}_{AsSb} < 8.3$ kcal/gfw and (2) that tetrahedrite-tennantites with intermediate Sb/(As + Sb) ratios have greater As/Sb ratios than the hydrothermal solutions from which they precipitated. The former inference is indicated by the observation that tetrahedrite-tennantites spanning the entire range of $X^{SM}_{Sb}/(X^{SM}_{As} + X^{SM}_{Sb})$ ratios are formed at temperatures as low as 250°C (e.g., Raabe and Sack, 1984). The latter inference is suggested by the observation that in paragenetic stages in hydrothermal veins in which tetrahedrite-tennantite is the only As- and Sb-bearing ore phase precipitated, it typically evolves towards greater $X^{SM}_{Sb}/(X^{SM}_{As} + X^{SM}_{Sb})$ ratios along the direction of flow of the mineralizing solutions. Because the Gibbs energies of appropriate tetrahedrite-tennantites are unknown, quantitative modelling of their compositional variations in epithermal deposits is premature. However, some constraints on As(Sb)$_{-1}$ exchange reactions between tetrahedrite-tennantites and hydrothermal fluids may be obtained by comparison of evaporative fractionation calculations for model tetrahedrite-tennantite-bearing solutions with compositional variation trends of tetrahedrite-tennantite in hydrothermal vein deposits. These calculations illustrate the important role that site interactions in the crystal play in influencing the downstream trends in chemical zoning of the ore deposit.

Hackbarth and Petersen (1984) have summarized composition zoning trends of tetrahedrite-tennantites from the Galena, Coeur, Sunshine, and Crescent mines in the Coeur d'Alene district in northern Idaho and from mines in the Casapalca, and Orcopampa districts in Peru. From their studies of effectively monomineralic crustification bands of tetrahedrite-tennantites, they have established probable temporal and spatial compositional zoning patterns, have identified Ag/(Ag + Cu) – Sb/(Sb + As) curves which enclose spatial composition zoning trends (Fig. 7), and have interpreted these zoning trends in terms of a general model of fractional crystallization. In their model it is assumed (1) that the As(Sb)$_{-1}$, Ag(Cu)$_{-1}$, and Zn(Fe)$_{-1}$ exchange reactions between tetrahedrite-tennantite and hydrothermal fluid are energetically independent, (2) that the distribution coefficients for As(Sb)$_{-1}$ and Ag(Cu)$_{-1}$ exchange between these phases,

$$K_{D1} \equiv \left(\frac{n^{TD-TN}_{Ag}}{n^{TD-TN}_{Cu}}\right)\left(\frac{m^{LIQ}_{Cu}}{m^{LIQ}_{Ag}}\right) = \left[\frac{X_4}{(1 - X_4) + 2/3}\right]\left(\frac{m^{LIQ}_{Cu}}{m^{LIQ}_{Ag}}\right) \quad (23)$$

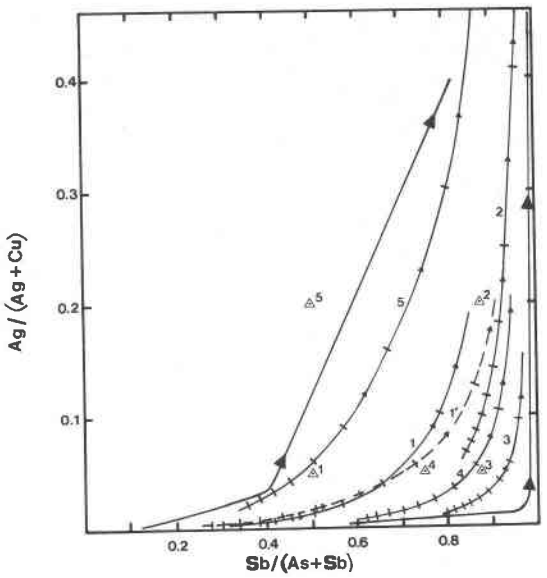

Fig. 7. Tetrahedrite-tennantite fractional crystallization curves expressed in terms of molar ratios Ag/(Ag + Cu) and Sb/(As + Sb). The initial metal and semimetal contents of the fluids are plotted as open triangles; these are 1 = $Ag_{0.5}Cu_{9.5}Fe_{0.5}Zn_{1.5}As_{2.0}Sb_{2.0}S_{13.0}$, 1' = $Ag_{0.5}Cu_{9.5}Fe_{1.5}Zn_{0.5}As_{2.0}Sb_{2.0}S_{13.0}$, 2 = $Ag_{2.0}Cu_{8.0}Fe_{0.5}Zn_{1.5}As_{0.5}Sb_{3.5}S_{13.0}$, 3 = $Ag_{0.5}Cu_{9.5}Fe_{0.5}Zn_{1.5}As_{0.5}Sb_{3.5}S_{13.0}$, 4 = $Ag_{0.5}Cu_{9.5}Fe_{0.5}Zn_{1.5}As_{1.0}Sb_{3.0}S_{13.0}$, and 5 = $Ag_{2.0}Cu_{8.0}Fe_{0.5}Zn_{1.5}As_{2.0}Sb_{2.0}S_{13.0}$. Tics on corresponding tetrahedrite-tennantite fractional crystallization curves indicate the fraction of the initial metals and semimetals crystallized, in increments of 0.1. In the calculations estimates of compositions of tetrahedrite-tennantite crystallized over 1/1000 step increments were obtained by averaging tetrahedrite-tennantite compositions calculated by iterative solution of equations (25)–(27) for the fluid composition at the beginning of the increment with that which would obtain if tetrahedrite-tennantite of this composition were crystallized over the entire increment. Values of T, $\Delta\bar{G}^{\circ}_{23}$, $\Delta\bar{G}^{\circ}_{24}$, $\Delta\bar{G}^{\circ}_{34}$, a/RT, b/RT, and c/RT used in these calculations were 260°C and 2.59, 3.00, 16.8, 0.0, −1.3, −0.6 kcal/gfw respectively. Tic-free curves represent the bounds on composition trends for tetrahedrite-tennantites from zoned vein deposits as given by Hackbarth and Petersen (1984). Arrows indicate the sense of downstream composition change in tetrahedrite-tennantite.

and

$$K_{D2} \equiv \left(\frac{n^{TD-TN}_{Sb}}{n^{TD-TN}_{As}}\right)\left(\frac{m^{LIQ}_{As}}{m^{LIQ}_{Sb}}\right) = \left[\frac{(1 - X_3)}{X_3}\right]\left(\frac{m^{LIQ}_{As}}{m^{LIQ}_{Sb}}\right), \quad (24)$$

are constant, (3) that surface equilibrium obtains between hydrothermal fluid and each successive batch of tetrahedrite-tennantite it crystallizes, (4) that after crystallization tetrahedrite-tennantites do not react with hydrothermal fluid, and (5) that changes in the composition of the hydrothermal fluid are due to the crystallization of tetrahedrite-tennantite alone. In their analysis Hackbarth and Petersen (1984) demonstrate that although both K_{D1} and K_{D2} must be less than unity to predict observed com-

position zoning trends from probable hydrothermal fluids, a wide range of values of K_{D1} and K_{D2} (between 0.1 and 0.9) are required for this purpose. The consistency between the observation that K_{D1} and K_{D2} are highly variable and the extents of energetic coupling among the $As(Sb)_{-1}$, $Ag(Cu)_{-1}$ and $Zn(Fe)_{-1}$ exchange reactions inferred on preceding pages is readily appreciated from inspection of the corresponding conditions of exchange equilibrium between tetrahedrite-tennantite and hydrothermal fluid written in an appropriate format for comparison with (23) and (24):

$$1/K_{D1} = \left[\frac{(5/3 - X_4)}{(1 - X_4)}\right] \cdot \exp\,[[a + 1/6(\Delta\bar{G}^{\circ}_{24}(X_2) + \Delta\bar{G}^{\circ}_{34}(X_3)]/RT], \quad (25)$$

$$K_{D2} = \exp\,[[b + 1/4(\Delta\bar{G}^{\circ}_{23}(X_2) + \Delta\bar{G}^{\circ}_{34}(X_4)]/RT] \quad (26)$$

and

$$K_{D3} \equiv \frac{(1 - X_2)}{X_2}\frac{m^{LIQ}_{Zn}}{m^{LIQ}_{Fe}} = \exp\,[[c + 1/2(\Delta\bar{G}^{\circ}_{23}(X_3) + \Delta\bar{G}^{\circ}_{24}(X_4)]/RT] \quad (27)$$

where the exchange potentials in the hydrothermal fluid are defined by the expressions

$$\mu^{LIQ}_{As(Sb)_{-1}} = \mu^{\circ LIQ}_{As(Sb)_{-1}} + RT\ln\left(\frac{m^{LIQ}_{As}}{m^{LIQ}_{Sb}}\right) + RT\ln\left(\frac{\gamma^{LIQ}_{As}}{\gamma^{LIQ}_{Sb}}\right), \quad (28)$$

$$\mu^{LIQ}_{Ag(Cu)_{-1}} = \mu^{\circ LIQ}_{Ag(Cu)_{-1}} + RT\ln\left(\frac{m^{LIQ}_{Ag}}{m^{LIQ}_{Cu}}\right) + RT\ln\left(\frac{\gamma^{LIQ}_{Ag}}{\gamma^{LIQ}_{Cu}}\right), \quad (29)$$

and

$$\mu^{LIQ}_{Zn(Fe)_{-1}} = \mu^{\circ LIQ}_{Zn(Fe)_{-1}} + RT\ln\left(\frac{m^{LIQ}_{Zn}}{m^{LIQ}_{Fe}}\right) + RT\ln\left(\frac{\gamma^{LIQ}_{Zn}}{\gamma^{LIQ}_{Fe}}\right), \quad (30)$$

a, b, and c are

$$a = 1/6(\mu^{\circ}_{Ag_6Cu_4Fe_2Sb_4S_{13}} - \mu^{\circ}_{Cu_{10}Fe_2Sb_4S_{13}}) - \left(\mu^{\circ LIQ}_{Ag(Cu)_{-1}} + RT\ln\left(\frac{\gamma^{LIQ}_{Ag}}{\gamma^{LIQ}_{Cu}}\right)\right), \quad (31)$$

$$b = 1/4(\mu^{\circ}_{Cu_{10}Fe_2As_4S_{13}} - \mu^{\circ}_{Cu_{10}Fe_2Sb_4S_{13}}) - \left(\mu^{\circ LIQ}_{As(Sb)_{-1}} + RT\ln\left(\frac{\gamma^{LIQ}_{As}}{\gamma^{LIQ}_{Sb}}\right)\right), \quad (32)$$

and

$$c = 1/2(\mu^{\circ}_{Cu_{10}Zn_2Sb_4S_{13}} - \mu^{\circ}_{Cu_{10}Fe_2Sb_4S_{13}}) - \left(\mu^{\circ LIQ}_{Zn(Fe)_{-1}} + RT\ln\left(\frac{\gamma^{LIQ}_{Zn}}{\gamma^{LIQ}_{Fe}}\right)\right), \quad (33)$$

and it has been assumed that tetrahedrite-tennantite is an "ideal" reciprocal solution.[5]

It is readily demonstrated that most of the downstream compositional variation trends exhibited by tetrahedrite-tennantites from essentially monomineralic crustification bands in zoned hydrothermal ore deposits may be reproduced by an heuristic fractionation model in which constant values of the coefficients a, b, and c in (25)–(27) are employed. In the simplest such model of perfect fractionation an average temperature ($T = 260°C$) is chosen, and tetrahedrite-tennantite is crystallized from solutions having ratios of the sums (Ag + Cu), (Fe + Zn), and (As + Sb) equal to those of the stoichiometric formula for "ideal" tetrahedrite-tennantite. The composition of tetrahedrite-tennantite crystallized at each step of fractionation is calculated by iterative solution of (25)–(27). Comparison of the results of trial calculations with space-time envelopes on Ag/(Ag + Cu) − Sb/(As + Sb) fractionation paths in zoned hydrothermal vein deposits (Hackbarth and Petersen, 1984) allows deduction of approximate values of a, b, and c.

Lacking quantitative fluid temperature–composition data, the schematic representation of aqueous species precludes recovery of exact values of the coefficients a, b, and c by this numerical simulation example, but it suggests several probable bounds on these coefficients. Because $\Delta\bar{G}^{\circ}_{34}$ and $\Delta\bar{G}^{\circ}_{23}$ are positive and the sense of downstream zoning requires that tetrahedrite-tennantites with intermediate Sb/(As + Sb) ratios have lower values of this ratio than the hydrothermal fluids that crystallize them, the coefficient b

[5] In order to preserve generality, relations (28)-(33) are represented in schematic form. It is well established that for the acidic brines implicated in formation of most hydrothermal silver-base metal sulfide deposits, chloride complexes of Ag, Cu, Zn, and possibly Fe are likely to predominate greatly over simple ions. Work by Helgeson (1969), Crerar and Barnes (1976), Seward (1976), and Crerar et al. (1978) indicate that over the range of salinities pertinent to these ore-forming solutions, the predominant chloride complexes of silver have higher ligand numbers than the predominant complexes of copper in the same solution, and zinc forms chloride complexes of higher ligand number than iron. Presently available data (Helgeson, 1969; Crerar et al., 1978) suggest that in a 2 molal NaCl solution at 260°C, Zn–Fe exchange between tetrahedrite-tennantite and predominant aqueous species might be described by

$$1/2Cu_{10}Fe_2Sb_4S_{13} + ZnCl_4^{-2} = 1/2Cu_{10}Zn_2Sb_4S_{13} + FeCl^{+} + 3Cl^{-},$$

in which case the Zn–Fe distribution coefficient for that fluid and tetrahedrite-tennantite could be recovered by setting $\mu^{\circ}_{Zn(Fe)_{-1}} = \mu^{\circ}_{ZnCl_4^{-2}} - \mu^{\circ}_{FeCl^{+}} - 3\mu^{\circ}_{Cl^{-}}$, the right-hand term would become $RT\ln(\gamma_{ZnCl_4^{-2}}/\gamma_{FeCl^{+}}\gamma^3_{Cl^{-}})$, and

$$c' = -RT\ln\frac{X_2}{1 - X_2}\frac{(m_{FeCl^{+}})(m^3_{Cl^{-}})}{m_{ZnCl_4^{-2}}}$$

The exchange distribution parameters a and c respond to salinity variations only to the extent that the *difference* in ligand numbers of the exchange pair varies with salinity.

in (26) must be negative. Values of b in the range of -1.0 to -1.5 kcal/gfw appear to give adequate fits to downstream covariation trends in Ag/(Ag + Cu) and Sb/(As + Sb) in tetrahedrite-tennantites from the Casapalca and Coeur d'Alene deposits for $a = c = 0$. Values of b in this range seem reasonable, because the form of tetrahedrite-tennantite Ag/(Ag + Cu) – Sb/(As + Sb) fractionation curves are fairly insensitive to values of c, and a must be a fairly small number in absolute value relative to the absolute value of b. For a given value of b, comparable values of a are not permitted because they lead to the development of unnatural negative correlations between Ag/(Ag + Cu) and Sb/(As + Sb) at advanced stages of crystallization of many of the tetrahedrite-tennantite bulk compositions investigated. Alternatively, positive values of a comparable in absolute value to b are not permitted because they do not allow duplication of the left-hand envelope on tetrahedrite-tennantite fractionation curves in Figure 7 for reasonable tetrahedrite-tennantite bulk compositions, by virtually excluding Ag from tetrahedrite-tennantite crystallized in the early stages of fractionation. To be consistent with the observation that virtually monomineralic tetrahedrite-tennantite fractionation paths in the Coeur d'Alene district do not exhibit prominent zoning in Zn/(Zn + Fe) (e.g., Hackbarth and Petersen, 1984), values of c must satisfy the inequality $b \leq c \leq 0$. Values of c near these lower and upper bounds lead to tetrahedrite-tennantite fractionation paths characterized respectively by decreasing and increasing Zn/(Zn + Fe) with increasing degree of crystallization.

Although, in detail, many of the assumptions of the model given above cannot be correct, even for stages of vein mineralization dominated by tetrahedrite-tennantite crystallization, agreement between spatial tetrahedrite-tennanite composition zoning trends observed in vein ore deposits and those predicted by the model suggests that it provides a useful paradigm. The conditions in the preceding calculations that are most unlikely to be fulfilled when applied to paragenetic stages of hydrothermal deposition are that only tennahedrite is crystallized and that the fluid has the ratios of (Ag + Cu)/(As + Sb) and (Fe + Zn)/(As + Sb) of tetrahedrite-tennantites with the "ideal" formula. In cases in which other sulfides are precipitated with tetrahedrite-tennantite, spatial zoning trends of tetrahedrite-tennantite will differ from those given by the model in a predictable manner. For example, where pyrite and sphalerite are coprecipitated with tetrahedrite-tennantite, the sulfidation trajectory will influence spatial zoning trends of (Fe/Zn) in tetrahedrite-tennantite, as a_{FeS} is reciprocally related to $\ln f_{S_2}$. Where arsenopyrite is coprecipitated with tetrahedrite-tennantite, the spatial variations of Ag/(Ag + Cu) versus Sb/(As + Sb) ratios tetrahedrite-tennantite will probably show enhanced concavity similar to curves 3 or 4 in Figure 7. Finally, coprecipitation of chalcopyrite will result in more positive concave upward slopes of tetrahedrite-tennantite fractionation curves than those displayed on Figure 7, because it will increase the Ag/Cu ratio of the fluid relative to that due to tetrahedrite-tennantite precipitation alone. In addition, as noted by Hackbarth and Petersen (1984), ratios of (Cu + Ag)/(As + Sb) in the fluid greater and less than those of tetrahedrite-tennantite with the "ideal" formula will yield tetrahedrite-tennantite fractionation paths characterized by smaller and greater slopes d(Ag/[Ag + Cu])/d(Sb/[As + Sb]), respectively. The remaining assumptions are less likely to result in serious discrepancies between tetrahedrite-tennantite fractionation paths observed in hydrothermal deposits and those predicted by the model.

Although exact precipitation mechanisms (e.g., cooling, dilution, boiling, change in chemistry by wallrock reaction, etc.) and fluid chemistries vary among and within deposits, tetrahedrite-tennantite zoning systematics along flowpaths are not likely to be sensitive to likely ranges of temperature or pH variations given the large relative magnitude of crystal energetic effects. However, due to differential complexing of metals with chloride in aqueous solutions, changes in fluid salinity along the flowpath (e.g., due to dilution or boiling) may strongly influence downstream zoning trends in mineral chemistry. For the exchange reaction

$$Cu_{10}Fe_2Sb_4S_{13} + 6AgCl_2^- = Ag_6Cu_4Fe_2Sb_4S_{13} + 6CuCl^\circ + 6Cl^-,$$

$$\frac{\partial \log [(X_4/X_1)^{TD}/(a_{AgCl^-}/a_{CuCl^\circ})^{LIQ}}{\partial \log a_{Cl^-}} = -1$$

Thus, for a fluid fractionally precipitating tetrahedrite-tennantite along its flow-path, isothermal dilution from 10.5 to 8.5 wt.% NaCl would tend to cause $(Ag/Cu)_{TD}^{TRG}$ to increase by 26%. Fluid inclusion studies have demonstrated that dilution of ascending metalliferous brines by heated, dilute groundwaters has been influential in the development of several tetrahedrite-tennantite-bearing, epithermal silver–base-metal vein deposits (e.g., Hayba, 1984; Robinson and Norman, 1984; Loucks, in prep.).

Although the hydrologic and chemical complexity of hydrothermal ore-forming processes present formidable challenges to quantitative interpretation of zoning trends in ore deposits, the zoning patterns may, on the other hand, be useful in discriminating the relative importance of a choice of operators. For example, thermochemical evaluation of model parameter c' for the case of a 2m NaCl solution at 260°C (see footnote 5), employing our value of 2.07 ± 0.07 kcal for the tetrahedrite–sphalerite Zn–Fe exchange potential, Crerar et al. (1978) for stabilities of ferrous chloride complexes, Helgeson (1969) for zinc chloride complexes and solubility products of sphalerite and troilite, Fleet (1975) for the conversion of FeS standard state from troilite to sphalerite structure, and using activity coefficients for aqueous complexes calculated according to Helgeson et al. (1981), predicts $(Fe/Zn)^{TD}(Fe/Zn)^{LIQ} \simeq 0.6$, which is in good agreement with constraints (0.5–0.8) obtained independently by iterative empirical fitting of a, b, and c parameters in (25)–(27) to Hackbarth and Petersen's (1984) trends of Ag–Cu, Zn–Fe, and Sb–As co-variation along nearly monomineralic tetrahedrite-tennantite parage-

netic stages of deep-seated veins in the Caspalca and Coeur d'Alene districts. According to Rye and Sawkins (1974), tetrahedrite-tennantite at Caspalca precipitated from fluids having 0.9–2.6 m NaCl-equivalent salinity, and Leach and Hofstra (1983) and Bijak and Norman (1983) report fluid salinities in the range 1.3–3.0 m NaCl-equivalent for tetrahedrite-tennantite bearing Coeur d'Alene veins. The crystal/fluid Fe/Zn partition ratio of ca. 0.6 calculated for a fluid of constant 2 m NaCl salinity (see footnote 5), considered together with the mutual interaction energies (equations 25–27), predicts the flat trend of downstream Zn–Fe zoning observed in these As–Ag-zoned deposits by Hackbarth and Petersen (1984) and Wu (1975). According to the Zn–Fe exchange reaction in footnote 5,

$$\frac{\partial \log [(X_{Zn}^{TET}/X_{Fe}^{TET})^{TN-TD}/(a_{ZnCl_4^{2-}}/a_{FeCl^+})^{LIQ}]}{\partial \log a_{Cl^-}} = -3$$

over moderate ranges of salinity variation, so failure to observe in those veins this rather dramatic downstream Zn/Fe zoning that should accompany substantial dilution or evaporation of ore fluids implies that downstream evolution of fluid salinity was not a significant factor in ore formation in those veins; rather, successive batches of fluid varied in salinity over the quoted range, but each batch retained its integrity downstream over the distance (>1 km) examined in the zoning studies. Such an inference from zoning trends with respect to operators inducing ore deposition would be in accord with the reported lack of evidence in fluid inclusions for H_2O evaporation during tetrahedrite-tennantite deposition at Casapalca or the Coeur d'Alene silver belt, and lack of evidence in fluid inclusion and quartz δD and $\delta^{18}O$ data for significant mixing of compositionally contrasting fluids during tetrahedrite-tennantite precipitation at Casapalca (Rye and Sawkins, 1974) or the Coeur d'Alene silver belt (Yates and Ripley, 1983).

Despite the physico-chemical complexity of hydrothermal mineralization processes, the agrement between predicted tetrahedrite-tennantite composition zoning trends (Fig. 7) and spatial zoning trends exhibited by tetrahedrite-tennantites precipitated in mineralization stages dominated by tetrahedrite-tennantite precipitation suggests that the inferences about the extents of energetic coupling between the $Ag(Cu)_{-1}$, $As(Sb)_{-1}$, and $Zn(Fe)_{-1}$ exchange reactions in tetrahedrite-tennantite are substantially correct, and that these effects are of sufficient magnitude that they exert a major control on tetrahedrite-tennantite fractionation trends.

Cu–Fe exchange equilibria

To this point we have explicitly assumed that most natural tetrahedrite-tennantites tend toward the "ideal" stoichiometry with 208 valence electrons per unit cell, a limiting stoichiometry consistent with both the requirements of an ionic model and the conditions for minimum energy suggested by a brillouin-zone model (e.g., Johnson and Jeanloz, 1983). Although this limiting stoichiometry may define an energy minimum, it does not represent a natural limit for the substitutions of Fe and Zn for Cu, because tetrahedrite-tennantites with both more and less than 208 valence electron per unit cell are found in nature (e.g., Charlat and Levy, 1974; Sandecki and Amcoff, 1981; Miller and Craig, 1983; Loucks, 1984) and are produced in the laboratory (e.g., Taksuka and Morimoto, 1977b; Sack and Loucks, 1983). Although both the ionic model and band theory predict that the vacancy-coupled substitutions $\square Fe(Cu_2)_{-1}$ and $\square Zn(Cu_2)_{-1}$ should govern deviations from the "ideal" stoichiometry, the experimental data suggest that large components of the $Fe(Cu)_{-1}$ and $Zn(Cu)_{-1}$ substitutions are required to explain deviations from the "ideal" formula towards copper-poor compositions, at least in tetrahedrite-tennantites in charges which did not form arsenopyrite. Therefore, the compositions of these tetrahedrite-tennantites are largely controlled by the conditions of $Fe(Cu)_{-1}$ and $Zn(Fe)_{-1}$ exchange equilibria, their compositions and thermodynamic properties may be described in terms of the mole fractions of the components $Cu_{10}Fe_2Sb_4S_{13}$, (X_1), $Cu_{10}Zn_2Sb_4S_{13}$, (X_2), $Cu_{10}Fe_2As_4S_{13}$, (X_3), and $Cu_9Fe_3Sb_4S_{13}$, (X_5), and, in principle, analysis of the conditions of $Fe(Cu)_{-1}$ exchange equilibrium among tetrahedrite-tennantite, ISS, and sphalerite should aid in assessing the effects that deviations from "ideal" stoichiometry have on the $Fe(Zn)_{-1}$ exchange reaction between tetrahedrite-tennantite and sphalerite.

Unfortunately, the Fe–Cu exchange equilibria involving tetrahedrite-tennantite, ISS, and sphalerite are unreversed and may therefore be used in a qualitative fashion only. Nevertheless, the distribution coefficient for $Fe(Cu)_{-1}$ exchange between tetrahedrite-tennantite and ISS is a simple function of X_2^{TD-TN} and X_5^{TD-TN} (see Fig. 8) or (Cu/Fe) ratio in ISS. In addition, approximate relative values of $\mu_{Fe(Cu)_{-1}}$ may be defined for charges containing ISS, sphalerite, and tennantite-tetrahedrite because ISS's (in tetrahedrite-bearing charges) and sphalerites are on the composition plane CuS–FeS–ZnS, to a close approximation. For example, graphical integration of the approximation

$$d\mu_{Fe(Cu)_{-1}} = \left[\left(\frac{X_{FeS}^{ISS} + X_{CuS}^{ISS}}{X_{CuS}^{ISS}}\right) - \left(\frac{X_{ZnS}^{ISS} X_{FeS}^{SPH}}{X_{CuS}^{ISS} X_{ZnS}^{SPH}}\right)\right] d\mu_{FeS}^{SPH} \qquad (34)$$

utilizing the a_{FeS}^{SPH}–X_{FeS}^{SPH} relations given by Fleet (1975) suggests that an upper bound on the average slope $d\mu_{Fe(Cu)_{-1}}/d\mu_{FeS}$ for the ISS-tetrahedrite-tennantite–sphalerite assemblage is about 2.6.[6] This bound suggests that ISS displays strong negative deviations from ideality with respect to the

[6] This approximation is the result of making the substitutions

$$d\mu_{ZnS}^{SPH} = -\left(\frac{X_{FeS}^{SPH}}{X_{ZnS}^{SPH}}\right) d\mu_{FeS}^{SPH} - \left(\frac{X_{CuS}^{SPH}}{X_{ZnS}^{SPH}}\right) d\mu_{CuS}^{SPH}$$

$$d\mu_{FeS}^{SPH} = d\mu_{FeS}^{ISS},$$

$$d\mu_{ZnS}^{SPH} = d\mu_{ZnS}^{ISS},$$

and $$d\mu_{CuS}^{SPH} = d\mu_{CuS}^{ISS}$$

into the Gibbs–Duhem equation for ISS, and neglecting the term

$$[(X_{ZnS}^{ISS} X_{CuS}^{SPH})/(X_{CuS}^{ISS} X_{ZnS}^{SPH})]\, d\mu_{CuS}^{SPH}$$

in the resulting expression.

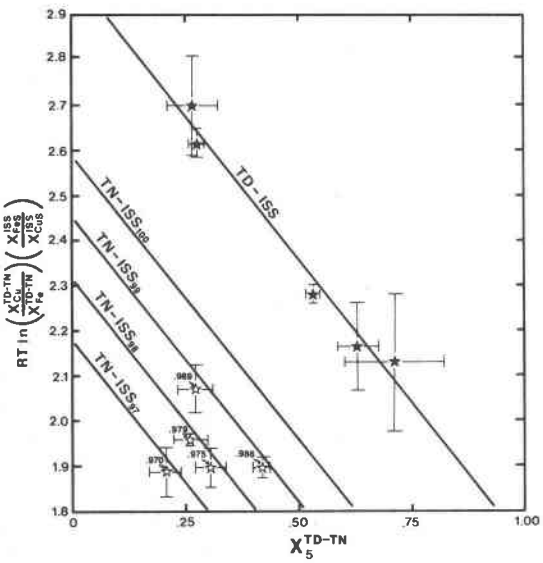

Fig. 8. RT ln K_c (kcal/gfw) as a function of X_5^{TD-TN} for tetrahedrite + ISS + sphalerite assemblages (solid stars) and "tennantite" + ISS + sphalerite assemblages (open stars) at 500°C. Error bars represent the standard errors associated with calculating RT ln K_c and X_5^{TD-TN} according to the following three assumptions consistent with the formula $Cu_{(10-X)}(Fe,Zn)_{2+X}(As,Sb)_4S_{13}$: (1) (Cu + Fe + Zn) = 12; $X_2 = (Zn/2)$; $X_5 = (10 - Cu)$, (2) (As + Sb) = 4; $X_2 = (Zn/2)$; $X_5 = (10 - Cu)$, and (3) S = 13; $X_2 = (Zn/2)$; $X_5 = (Fe + Zn - 2)$. The calibration of (36) for Cu-Fe exchange between ISS and tetrahedrite is based on the values of $\Delta\bar{G}_c^\sigma$, W_{CuFe}^{TET}, and W_{CuFe}^{ISS}, and $[2(W_{CuFe}^{TET} - W_{CuZn}^{TET}) + 1/2\ W_{FeZn}^{TET}]$ of 2.36, 0.64, 0.00 and 0.00 kcal/gfw. Calibration of (36) for Cu-Fe exchange between tennantite and As-free ISS is based on a value of $\Delta\bar{G}_{35}^\circ = -0.40$ kcal/gfw obtained by utilizing the values of W_{CuFe}^{TET}, W_{CuFe}^{ISS}, and $\Delta\bar{G}_c^\sigma$ given above and the following empirical correction for the effect of the As/(As + S) ratio of ISS on RT ln K_c:

$$RT \ln K_c = RT \ln K_c^* + B(As/[As + S])^{ISS}$$

where K_c and K_c^* represent tennantite + ISS + sphalerite assemblages which have As-free and As-bearing ISS, respectively, and the value of B defined by the experimental data is +13.77 kcal/gfw. Numbers adjacent to data points for tennantite-ISS assemblages give the S/(As + S) ratio of the ISS.

mixing of Cu and Fe. The inferred stabilization of coupled Cu and Fe substitutions on adjacent sites in ISS is supported by the formation of several ordered compounds (e.g., chalcopyrite and cubanite) on the FeS–CuS join; the deduction that $W_{ZnCu}^{TET} > W_{FeZn}^{TET} \sim 0 \geq W_{FeCu}^{TET}$ would be consistent with the observed topology of sphalerite-ISS tielines on the CuS–FeS–ZnS composition plane (e.g., Kojima and Sugaki, 1984; Fig. 3) if it were assumed that the thermodynamic properties of such ISS's and sphalerites exhibit ternary regular solution behavior.

In addition, the upper bounds on relative values of $\mu_{Fe(Cu)_{-1}}$ provided by graphical integration of (34) suggest that tetrahedrites may exhibit slight negative deviations from ideality with respect to $Fe(Cu)_{-1}$ exchange. Following the procedures and assumptions about site occupancies given above, we may write the following expressions for the distribution coefficients for $Zn(Fe)_{-1}$ and $Fe(Cu)_{-1}$ exchange between Ag-free tetrahedrite-tennantite and sphalerite, and between Ag-free tetrahedrite-tennantite and ISS:

$$RT \ln K_D = \Delta\bar{G}^\circ_{Zn(Fe)_{-1}} + \frac{\Delta\bar{G}^\circ_{23}}{2}(X_3) + RT \ln\left(\frac{\gamma_{FeS}^{SPH}}{\gamma_{ZnS}^{SPH}}\right) + \frac{W_{FeZn}^{TET}}{2}(1 - 2X_2) + [(W_{CuFe}^{TET} - W_{CuZn}^{TET}) + 1/4\ W_{FeZn}^{TET}](X_5) \quad (35)$$

and

$$RT \ln K_c = RT \ln\left[\left(\frac{X_{Cu}^{TET}}{X_{Fe}^{TET}}\right)^{TD-TN}\left(\frac{X_{FeS}^{ISS}}{X_{CuS}^{ISS}}\right)\right] = \Delta\bar{G}_c^\sigma + \Delta\bar{G}_{35}^\circ(X_3) + W_{CuFe}^{TET}(1 - 2X_5) + [2(W_{CuFe}^{TET} - W_{CuZn}^{TET}) + 1/2\ W_{FeZn}^{TET}] \cdot (X_2) - W_{CuFe}^{ISS}(1 - 2X_{FeS}^{ISS}) \quad (36)$$

where

$$\Delta\bar{G}_c^\sigma = (\bar{G}^\circ_{CuS} - \bar{G}^\circ_{FeS}) + (\bar{G}^*_{Cu_9Fe_3Sb_4S_{13}} - \bar{G}^*_{Cu_{10}Fe_2Sb_4S_{13}}) + (W_{CuZn}^{ISS} - W_{CuFe}^{ISS} - W_{FeZn}^{ISS})(X_{ZnS}^{ISS}) \quad (37)$$

and

$$\Delta\bar{G}_{35}^\circ = (\bar{G}^\circ_{Cu_9Fe_3As_4S_{13}} + \bar{G}^\circ_{Cu_{10}Fe_2Sb_4S_{13}}) - (\bar{G}^\circ_{Cu_9Fe_3Sb_4S_{13}} + \bar{G}^\circ_{Cu_{10}Fe_2As_4S_{13}}). \quad (38)$$

It may be readily shown that the inferences that $W_{CuFe}^{TET} < 0$, $W_{FeZn}^{TET} \sim 0$, and $W_{CuZn}^{TET} \geq 0$ would be consistent with (35) and the observation that the experimental data suggest more negative values of the derivative $RT(\mathrm{d} \ln K_D/\mathrm{d}\ X_{FeS}^{SPH})$ with increasing X_3, because the derivatives $\mathrm{d}X_2/\mathrm{d}X_{FeS}$ are about equal for tetrahedrites, tetrahedrite-tennantites and tennatites but $\mathrm{d}X_5^{TD}/\mathrm{d}X_{FeS}^{SPH} > \mathrm{d}X_5^{TD-TN}/\mathrm{d}X_{FeS}^{SPH} > \mathrm{d}X_5^{TN}/\mathrm{d}X_{FeS}^{SPH}$. Similarly analysis of ISS + tetrahedrite-tennantite assemblages utilizing (34) suggests that $\Delta\bar{G}_{35}^\circ$ is slightly negative (Fig. 8). However, given the uncertainties in all of the above, we consider that the presently available data do not provide a compelling case for adoption of an assumption other than that

$$\Delta\bar{G}_{35}^\circ \simeq W_{CuFe}^{TET} \simeq W_{FeZn}^{TET} \simeq W_{CuZn}^{TET} \simeq 0 \quad (39)$$

Discussion

From the preceding analysis, it is apparent that tetrahedrite-tennantite sulfosalts rank among the true "Cadillacs" of reciprocal solutions, have the potential to be among the most important of petrogenetic indicators of hydrothermal mineralization environments in polymetallic base-metal sulfide and bonanza precious metal deposits, and, despite their structural and chemical complexity, are remarkably well behaved energetically. It has been inferred that, to an excellent first approximation, the energetic coupling between the three principal substitutions on the metal and semimetal sites in tetrahedrite-tennantites—

$(Ag\rightleftharpoons Cu)^{TRG}$, $(Fe\rightleftharpoons Zn)^{TET}$, and $(As\rightleftharpoons Sb)^{SM}$, respectively—may be simply described in terms of an "ideal" reciprocal solution model (e.g., Wood and Nicholls, 1978; Sack, 1982) with values of 2.59 ± 0.14, 3.0 ± 1.5, and 16.8 ± 5.0 kcal/gfw for the standard state Gibbs energies of reciprocal reactions (7)–(9). The inferences that $\Delta\bar{G}^\circ_{23} \sim \Delta\bar{G}^\circ_{24}$ and $\Delta\bar{G}^\circ_{34} \gg \Delta\bar{G}^\circ_{23}$ may be readily rationalized crystallographically. Structure refinements of tetrahedrite-tennantites (Wuench, 1964; Wuench et al., 1966; Kalbskopf, 1972; Johnson and Burnham, 1985; Peterson and Miller, 1985) indicate that both the $Ag(Cu)_{-1}$ and $As(Sb)_{-1}$ exchanges produce slight compression and increasing regularity in shape of the tetrahedral metal site (Cu(1)) and a decrease in the size of the pyramid defined by semimetal–sulfur linkages. However, these substitutions have opposing effects on the trigonal-planar metal sites containing Ag and Cu (Cu(2)); the $Ag(Cu)_{-1}$ and $As(Sb)_{-1}$ exchanges respectively increase and decrease the areas available for metal coordination and anisotropic thermal motion. Because the changes in metal–sulfur distances due to these exchanges are significantly larger for Cu(2) metals than for Cu(1) metals, and Ag^+ has a larger radius than Cu^+ in trigonal coordination by sulfur (Shannon, 1981), a large value of $\Delta\bar{G}^\circ_{34}$ relative to $\Delta\bar{G}^\circ_{24}$ and $\Delta\bar{G}^\circ_{23}$ is consistent with these crystallographic data.

Although the data examined suggest that tetrahedrite-tennantites may be remarkably simple energetically, it is clear that many uncertainties in their thermodynamic properties need to be addressed before they may be used to place quantitative constraints on ore forming processes. In particular, it will be necessary to characterize the thermodynamic properties of at least one endmember tetrahedrite-tennantite before quantitative mass-transfer calculations may be attempted (e.g., Helgeson and Murphy, 1983). In addition, there are presently large uncertainties in $\Delta\bar{G}^\circ_{24}$ and $\Delta\bar{G}^\circ_{34}$ and the partial derivatives $\partial\Delta\bar{G}^\circ_{24}/\partial T$, $\partial\Delta\bar{G}^\circ_{34}/\partial T$, and $\partial\Delta\bar{G}^\circ_{Zn(Fe)_{-1}}/\partial T$. Even though the experimental results indicate that deviations from thermodynamic ideality due to the Fe⇌Zn substitution may be negligible, deviations from ideality due to the substitutions As⇌Sb and Ag⇌Cu in semimetal and trigonal-planar sites have yet to be quantified. Uncertainties in $\Delta\bar{G}^\circ_{24}$ and $\Delta\bar{G}^\circ_{34}$ derive, in part, from uncertainties in the structural role of silver in tetrahedrite-tennantites and the paucity of phase-petrologic studies on the appropriate natural assemblages. Although the analysis given here suggests that deviations from ideality due to the As⇌Sb and Ag⇌Cu substitutions may be small, this suspicion cannot be advanced with certainty until the appropriate experiments and/or phase petrologic studies of the critical natural assemblages are performed. Lastly, the bonding mechanisms in tetrahedrite-tennantites are poorly understood (e.g., Johnson and Jeanloz, 1983; Jeanloz and Johnson, 1984). It is anticipated that further characterization of the Gibbs energies of reciprocal reactions in Mn-, Cd-, Hg-, and Bi-bearing tetrahedrite-tennantites may provide additional insights into bonding mechanisms.

Despite present uncertainties in the analysis of the thermodynamic properties of tetrahedrite-tennantites, it is clear that they should be useful in refining the thermochemical interpretations of many ore-forming environments due to their capacity for a wide range of substitutions of semimetals and metals and adjustable stoichiometry. Given the thermodynamic properties of tetrahedrite-tennantites and ions in hydrothermal fluids, salinity and temperature data from fluid inclusions, and specification of the activities of one or more elements or ions through mineral–fluid equilibria, the composition of tetrahedrite-tennantites could be used to define the concentrations of many base metal and semimetal ions in the hydrothermal fluid. Combined with models for hydrothermal transport coupled with chemical reaction (e.g., Lichtner, 1985), such information would be invaluable in assessing precipitation mechanisms and mineralization potential in silver-bearing base-metal sulfide deposits of hydrothermal origin. Even in the absence of all the requisite information for this purpose, studies of compositional zoning in tetrahedrite-tennantites provide a basis for establishing spatial and temporal trends in metal and semimetal ratios of hydrothermal fluids and assessing models of ore deposition. Studies of metal ratios and compositional zoning in tetrahedrite-tennantite offer significant promise as guides to exploration and mine development, where variations in metal ratios in tetrahedrite-tennantite parallel those in bulk ore samples or tetrahedrite-tennantite is the principal ore phase (e.g., Goodell and Petersen, 1974; Petersen et al., 1977; Wu and Petersen, 1977; Hackbarth and Petersen, 1984). For example, in cases where silver mineralization is dominated by tetrahedrite-tennantite crystallization, fractionation calculations of the type illustrated in Figure 7 might be compared with metal ratio maps for bulk ore samples to predict grades as well as locations of undiscovered ore in a partially developed district.

Summary

Experimental constraints, petrologic studies, and theoretical analysis suggest that, energetically, tetrahedrite-tennantite sulfosalts are remarkably well behaved multisite reciprocal solutions. Fe–Zn exchange experiments (500°C) between tetrahedrite-tennantites and sphalerites yield values of 2.59 ± 0.14 and 2.07 ± 0.07 kcal/gfw for the Gibbs energies of the reciprocal reaction

$$Cu_{10}Zn_2Sb_4S_{13} + Cu_{10}Fe_2As_4S_{13} = Cu_{10}Fe_2Sb_4S_{13} + Cu_{10}Zn_2As_4S_{13}$$

and Fe–Zn exchange reaction

$$1/2\ Cu_{10}Fe_2Sb_4S_{13} + ZnS = 1/2\ Cu_{10}Zn_2Sb_4S_{13} + FeS,$$

respectively. These results, plus petrologic studies of tetrahedrite-tennantite + sphalerite assemblages, and preliminary experimental results at 435 and 365°C suggest that the above parameters are insensitive to temperature and permit estimates for the Gibbs energies of the remaining two reciprocal reactions of "ideal" tetrahedrite tennantites ($(Ag,Cu)_6Cu_4(Fe,Zn)_2(As,Sb)_4S_{13}$): $Cu_{10}Zn_2Sb_4S_{13} + Ag_6Cu_4Fe_2Sb_4S_{13} = Cu_{10}Fe_2Sb_4S_{13} + Ag_6Cu_4Zn_2Sb_4S_{13}$ and $Ag_6Cu_4Fe_2Sb_4S_{13} + Cu_{10}Fe_2As_4S_{13} =$

$Cu_{10}Fe_2Sb_4S_{13}$ + $Ag_6Cu_4Fe_2As_4S_{13}$ of 3.0 ± 1.5 and 17 ± 5 kcal/gfw, respectively.

These considerations suggest that tetrahedrite-tennantites are the "Cadillac" of reciprocal solutions and of petrogenetic indicators of hydrothermal mineralizing environments; they are the sulfide analog of amphiboles, the "Rolls Royce" of reciprocal solutions and petrogenetic indicators. In addition to providing a means for deducing aspects of the chemistry of many hydrothermal mineralizing fluids, our results afford an improved basis for understanding downstream chemical zoning in polymetallic base-metal sulfide and bonanza precious metal deposits. In particular they provide strong evidence that crystallochemical control coupled with As–Sb fractionation determines the distribution of silver in many zoned Pb–Zn–Cu–Ag deposits.

Acknowledgments

We thank the following individuals for their many and varied contributions to this study: P. B. Barton, Jr., G. Brimhall, J. K. Bohlke, S. E. Bushnell, I. S. E. Carmichael, D. Ebel, V. G. Ewing, D. Foss, J. F. Hays, C. J. Hackbarth, H. C. Helgeson, M. L. Johnson, G. Kullerud, D. W. Levandowski, P. C. Lichtner, M. J. O'Leary, U. Petersen, K. C. Raabe, S. L. Rogal, J. B. Thompson, Jr., D. Walker, and B. J. Wood. In particular we thank P. B. Barton, Jr., M. Johnson, G. Kullerud, and B. J. Wood for their helpful reviews, I. S. E. Carmichael for arranging access to the microprobe of the University of California, J. F. Hays for arranging for initial funding, M. Johnson for monitoring furnace temperatures and rescuing the experimental charges from a wastebasket in the Hoffman Laboratory of Experimental Geology, and U. Petersen for sharing data in advance of publication and stimulating our initial interest in the problem. R. O. Sack acknowledges the support of NSF grants EAR-82-18286 and EAR-84-19185, U.S. Bureau of Mines grant G114411, and a travel grant from the Department of Geosciences, Purdue University. R. R. Loucks acknowledges a COFRS grant from Florida State University.

References

Barton, P. B., Jr. (1978) Some ore textures involving sphalerite from Furutobe mine, Akita Prefecture, Japan. Mining Geology, 28, 293–300.

Barton, P. B., Jr., Bethke, P. M., and Toulmin, Priestley, III (1963) Equilibrium in ore deposits. Mineralogical Society of America Special Paper 1, IMA Papers, Third General Meeting, 171–185.

Barton, P. B., Jr. and Skinner, B. J. (1979) Sulfide mineral stabilities. In H. L. Barnes, Ed., Geochemistry of Hydrothermal Ore Deposits, 2nd Ed., p. 278–403. Wiley, New York.

Barton, P. B., Jr. and Toulmin, Priestley, III (1966) Phase relations involving sphalerite in the Fe–Zn–S system. Economic Geology, 61, 815–849.

Bijak, M. K. and Norman, D. I. (1983) Mineraliation of the Bunker Hill mine, Coeur d'Alene district, Idaho, in light of fluid inclusion studies. Geological Society of America Abstracts with Program, 15, 443.

Boorman, R. S. (1967) Subsolidus studies in the ZnS–FeS–FeS_2 system. Economic Geology, 62, 614–631.

Bushnell, S. E. (1983) Paragenesis and zoning of the Cananea-Duluth Breccia Pipe, Sonora, Mexico. Ph.D. Thesis, Harvard University, Cambridge, Massachusetts.

Cabri, L. J. (1973) New data on phase relations in the Ce–Fe–S system. Economic Geology, 68, 443–454.

Charlat, Michael and Levy, Claude (1974) Substitutions multiples dans la serie tennantite-tetraedrite. Bulletin de la Société francaise de Minéralogie et de Cristallographie, 97, 241–250.

Charlat, Michael and Levy, Claude (1975) Influence principales sur le parametre cristallin dans la serie tennantite-tetrahedrite. Bulletin de la Société francaise de Minéralogie et de Cristallographie, 98, 152–158.

Colby, J. W. (1972) MAGIC IV—a computer program for quantitative electron microprobe analysis: Papers with Program, Electron Probe Analysis Society American Tutorial Session, 7th National Conference on Electron Probe Analysis, San Francisco, Bal–Bal6.

Craig, J. R. and Barton, P. B., Jr. (1973) Thermochemical approximations for sulfosalts. Economic Geology, 68, 493–506.

Crerar, D. A. and Barnes, H. L. (1976) Ore solution chemistry V. Solubilities of chalcopyrite and chalcocite assemblages in hydrothermal solution at 200° to 350°C. Economic Geology, 71, 772–794.

Crerar, D. A., Susak, N. J., Borcsik, M., and Schwartz, S. (1978) Solubility of the buffer assemblage pyrite + pyrrhotite + magnetite in NaCl solutions from 200 to 350°C. Geochimica et Cosmochimica Acta, 42, 1427–1437.

Czamanske, G. K. and Hall, W. E. (1975) The Ag–Bi–Pb–Sb–S–Se–Te mineralogy of the Darwin lead–silver–zinc deposit, southern California. Economic Geology, 70, 1092–1110.

Darken, L. S. and Gurry, R. W. (1953) Physical Chemistry of Metals. McGraw-Hill, New York.

Einaudi, M. T. (1977) Environment of ore deposition at Cerro De Pasco, Peru. Economic Geology, 893–924.

Eldridge, C. S., Barton, P. B., Jr., and Ohmoto, Hiroshi (1983) Mineral textures and their bearing on formation of the kuroko orebodies. In H. Ohmoto and B. J. Skinner, Eds., The Kuroko and Related Volcanogenic Massive Sulfide Deposits: Economic Geology Monograph 5, 241–281.

Fleet, M. E. (1975) Thermodynamic properties of (Zn,Fe)S solid solutions at 850°C. American Mineralogist, 60, 466–470.

Goodell, P. C. and Petersen, Ulrich (1974) Julcani mining district, Peru: A study of metal ratios. Economic Geology, 69, 347–361.

Hackbarth, C. J., Petersen, Ulrich, and others (1981) Zoning analysis applied to the argentian tetrahedrite veins of Orcopampa, Peru and Coeur d'Alene, Idaho. Program handout, Harvard Mining Geology Seminar, April, 1981.

Hackbarth, C. J. and Petersen, Ulrich (1983) Compositional variations in hydrothermal tetrahedrites—an ore depositional model. Geological Society of America Abstracts with Programs, 15, 588.

Hackbarth, C. J. and Petersen, Ulrich (1984) Systematic compositional variations in argentian tetrahedrite. Economic Geology, 79, 448–460.

Hall, A. J. (1972) Substitution of Cu by Zn, Fe, and Ag in synthetic tetrahedrite. Bulletin de la Société francaise de Minéralogie et de Petrologie, 95, 583–594.

Hayba, D. O. (1984) Documentation of thermal and salinity gradients and interpretation of the hydrologic conditions in the OH vein, Creede, Colorado. Geological Society of America Abstracts with Program, 16, 534.

Helgeson, H. C. (1969) Thermodynamics of hydrothermal systems at elevated temperatures and pressures. American Journal of Science, 267, 729–804.

Helgeson, H. C., Kirkham, D. H., and Flowers, G. C. (1981) Theoretical prediction of the thermodynamic behavior of aqueous electrolytes at high pressures and temperatures: IV. Calculations of activity coefficients, osmotic coefficients, and apparent molal and standard and relative partial molal properties to 600°C and 5 kb. American Journal of Science, 281, 1249–1516.

Helgeson, H. C. and Murphy, W. M. (1983) Calculation of mass transfer among minerals and aqueous solutions as a function of time and surface area in geochemical processes. I. Computational approach. Mathematical Geology, 15, 109–130.

Hellner, Erwin (1958) A structural scheme for sulfide minerals. Journal of Geology, 66, 503–525.

Hobbs, S. W. and Fryklund, V. C. (1968) The Coeur d'Alene district, Idaho. In J. D. Ridge, Ed., Ore Deposits of the United States, Graton-Sales Volume, v. 2, 1417–1435.

Hutchison, M. N. and Scott, S. D. (1981) Sphalerite geobarometry in the Cu–Fe–Zn–S system. Economic Geology, 76, 143–153.

Jeanloz, Raymond and Johnson, M. L. (1984) A note on the bonding, optical spectrum and composition of tetrahedrite. Physics and Chemistry of Minerals, 11, 52–54.

Johnson, M. L. and Burnham, C. W. (1985) Crystal structure refinement of an arsenic-bearing argentian tetrahedrite. American Mineralogist, 70, 165–170.

Johnson, M. L. and Jeanloz, Raymond (1983) A brillouin-zone model for compositional variation in tetrahedrite. American Mineralogist, 68, 220–226.

Kalbskopf, R. (1971) Die Koordination des Quicksilbers im Schwazit. Tschermaks Mineralogisch und Petrographische Mitteilungen, 16, 173–175.

Kalbskopf, R. (1972) Strukturverfeinerung des freibergits. Tschermaks Mineralogisch und Petrographische Milleilungen, 18, 147–155.

Kane, F. J. and Petersen, Ulrich (1985) Tetrahedrite and bulk ore zoning in the Mimosa section of Julcani, Peru. Economic Geology.

Kojima, Shoji and Sugaki, Asahiko (1984) Phase relations in the central portion of the Cu–Fe–Zn–S system between 800° and 500°C. Mineralogical Journal, 12, 15–28.

Knight, J. E. (1977) A thermochemical study of alunite, enargite, luzonite, and tennantite deposits. Economic Geology, 72, 1321–1336.

Kullerud, Gunnar (1953) The FeS–ZnS system, a geological thermometer. Norsk Geologisk Tiddsskrift, 32, 61–147.

Kullerud, Gunnar, (1971) Experimental methods in dry sulfide research. In G. C. Ulmer, Ed., Research Techniques for High Pressure and High Temperature, p. 288–315. Springer-Verlag, New York.

Leach, D. L. and Hofstra, A. H. (1983) Fluid inclusion studies in the Coeur d'Alene district, Idaho. Geological Society of America Abstracts with Program, 15, 327.

Lichtner, P. C. (1985) Continuum model for simultaneous chemical reactions and mass transport in hydrothermal systems. Geochimica Cosmochimica Acta (in press).

Loucks, R. R. (1984) Zoning and ore genesis at Topia, Durango, Mexico. Ph.D. Thesis, Harvard University, Cambridge, Massachusetts.

Luce, F. D., Tuttle, C. L., and Skinner, B. J. (1977) Studies of sulfosalts of copper, V. Phases and phase relations in the system Cu–Sb–As–S between 350° and 500°C. Economic Geology, 72, 271–289.

Makovicky, Emil and Skinner, B. J. (1978) Studies of the sulfosalts of copper. VI. Low-temperature exsolution in synthetic-tetrahedrite solid solution; $Cu_{12+x}Sb_{4+y}S_{13}$. Canadian Mineralogist, 16, 611–623.

Makovicky, Emil and Skinner, B. J. (1979) Studies of the sulfosalts of copper. VII. Crystal structures of the exsolution products $Cu_{12.3}Sb_4S_{13}$ and $Cu_{13.8}Sb_4S_{13}$ of unsubstituted synthetic tetrahedrite. Canadian Mineralogist, 17, 619–634.

Maske, Siegfried and Skinner, B. J. (1971) Studies of the sulfosalts of copper. I. Phase and phase relations in the system Cu–As–S. Economic Geology, 66, 901–918.

McLimans, R. K., Barnes, H. L., and Ohmoto, Hiroshi (1980) Sphalerite stratigraphy of the Upper Mississippi Valley zinc-lead district, southwest Wisconsin. Economic Geology, 75, 351–361.

Miller, J. W. and Craig, J. R. (1983) Tetrahedrite-tennantite series compositional variations in the Cofer deposit, Mineral District, Virginia. American Mineralogist, 68, 227–234.

Nowacki, Werner (1969) Zur klassifikation and kristallochemie der sulfosalze. Schweizerische Mineralogische und Petrographische Mitteilungen, 49, 109–156.

Pattrick, R. A. D. (1978) Microprobe analyses of cadmium-rich tetrahedrites from Tyndrum, Perthshire, Scotland. Mineralogical Magazine, 42, 286–288.

Pattrick, R. A. D. and Hall, A. J. (1983) Silver substitution into synthetic zinc, cadmium, and iron tetrahedrites. Mineralogical Magazine, 47, 441–451.

Pauling, Linus and Neuman, E. W. (1934) The crystal structure of binnite, $(Cu,Fe)_{12}As_4S_{13}$, and the chemical composition and structure of minerals in the tetrahedrite group. Zeitschrift für Kristallographie, 88, 54–62.

Petersen, Ulrich, Noble, D. C., Arenas, M. J., and Goodell, P. C. (1977) Geology of the Julcani mining district, Peru. Economic Geology, 72, 931–949.

Pisutha-Arnond, V. and Ohmoto, Hiroshi (1983). Thermal history and chemical and isotopic compositions of the ore-forming fluids responsible for the kuroko massive sulfide deposits in the Hokuroku district of Japan. In Hiroshi Ohmoto, and B. J. Skinner, Eds., The Kuroko and Related Volcanogenic Massive Sulfide Deposits: Economic Geology Monograph 5, 523–558.

Raabe, K. C. and Sack, R. O. (1984) Growth zoning in tetrahedrite-tennantite from the Hock Hocking mine, Alma, Colorado. Canadian Mineralogist, 22, 577–582.

Riley, J. F. (1974) The tetrahedrite-freibergite series, with reference to the Mount Isa Pb–Zn–Ag ore body. Mineralium Deposita, 9, 117–124.

Robinson, R. W. and Norman, D. I. (1984) Mineralogy and fluid inclusion study of the southern Amethyst vein system, Creede mining district, Colorado. Economic Geology, 79, 439–447.

Rye, R. O. and Sawkins, F. J. (1974) Fluid inclusion and stable isotope studies on the Casapalca Ag–Pb–Zn–Cu deposit, central Andes, Peru. Economic Geology, 69, 181–205.

Sack, R. O. (1980) Some constraints on thermodynamic mixing properties of Fe–Mn olivines and orthopyroxenes. Contributions to Mineralogy and Petrology, 71, 257–269.

Sack, R. O. (1982) Spinels as petrogenetic indicators: activity-composition relations at low pressures. Contributions to Mineralogy and Petrology, 79, 169–186.

Sack, R. O., Carmichael, I. S. E. (1984) $Fe^{2+} \rightleftharpoons Mg^{2+}$ and $TiAl_2 \rightleftharpoons (MgSi_2)_{-1}$ exchange reactions between clinopyroxenes and silicate melts. Contributions to Mineralogy and Petrology, 85, 103–115.

Sack, R. O. and Loucks, R. R. (1983) Exchange experiments between sphalerites and tetrahedrite-tennantite solid solutions. Geological Society of America Abstracts with Programs, 15, 676–677.

Sandecki, J. and Amcoff, O. (1981) On the occurrence of silver-rich tetrahedrite at Garpenberg Norra, Central Sweden. Neues Jahrbuch für Mineralogie, Abhandlungen, 141, 324–340.

Scott, S. D. and Barnes, H. L. (1971) Sphalerite geothermometry and geobafometry. Economic Geology, 66, 653–669.

Seward, T. M. (1976) The stability of chloride complexes of silver in hydrothermal solutions up to 350°C. Geochimica et Cosmochimica Acta, 40, 1329–1341.

Shannon, R. D. (1981) Bond distances in sulfides and a preliminary table of sulfide crystal radii. In Michael O'Keeffe and Alex-

andra Navrotsky, Eds., Structure and Bonding in Crystals 2, p. 53–70. Academic Press, New York.

Shimazaki, Y. (1974) Ore minerals of the kuroko-type deposits. In S. Ishihara, Ed., Geology of the Kuroko Deposits: Mining Geology Special Issue 6, 311–322.

Skinner, B. J., Luce, F. D., and Makovicky, Emil (1972) Studies of the sulfosalts of copper, III. Phases and phase relations in the system Cu–Sb–S. Economic Geology, 67, 924–938.

Springer, G. (1969) Electron probe analyses of tetrahedrite. Neues Jahrbuch für Mineralogie, Monatshefte, 24–32.

Takeucki, Yoshio and Sadanago, Ryoichi (1969) Structural principles and classification of sulfosalts. Zeitschrift für Kristallographie, 130, 346–368.

Tatsuka, Kiyoaki and Morimoto, Nobuo (1973) Composition variation and polymorphism of tetrahedrite in the Cu–Sb–S system below 400°C. American Mineralogist, 58, 425–434.

Tatsuka, Kiyoaki and Morimoto, Nobuo (1977a) Tetrahedrite stability relations in the Cu–Sb–S system. Economic Geology, 72, 258–270.

Tatsuka, Kiyoaki and Morimoto, Nobuo (1977b) Tetrahedrite stability relations in the Cu–Fe–Sb–S system. American Mineralogist, 62, 1101–1109.

Thompson, J. B., Jr. (1969) Chemical reactions in crystals. American Mineralogist, 54, 341–375.

Thompson, J. B., Jr. and Thompson, A. B. (1976) A model system for mineral facies in pelitic schists. Contributions to Mineralogy and Petrology, 58, 243–277.

Toulmin, Priestley, III and Barton, P. B., Jr. (1964) A thermodynamic study of pyrite and pyrrhotite. Geochimica et Cosmochimica Acta, 28, 641–671.

Weissberg, B. G., Browne, P. R. L., and Seward, T. M. (1979) Ore metals in active geothermal systems. In H. L. Barnes, ed., Geochemistry of Hydrothermal Ore Deposits, 2nd ed., p. 738–780. Wiley, New York.

White, D. E., Anderson, E. T., and Grubbs, D. K. (1963) Geothermal brine well: mile-deep drill hole may tap ore-forming magmatic water rocks undergoing metamorphism. Science, 139, 919–922.

Wood, B. J. and Nicholls, James (1978) The thermodynamic properties of reciprocal solid solutions. Contributions to Mineralogy and Petrology, 66, 389–400.

Wu, Ishiung (1975) Geochemistry of tetrahedrite-tennantite at Casapalca, Peru. Ph.D. dissertation, Harvard University.

Wu, Ishiung and Peterson, Ulrich (1977) Geochemistry of tetrahedrite and mineral zoning at Casapalca, Peru. Economic Geology, 72, 993–1016.

Wuensch, B. J. (1964) The crystal structure of tetrahedrite, $Cu_{12}Sb_4S_{13}$. Zeitschrift für Kristallographie, 119, 437–453.

Wuensch, B. J., Takeuchi, Yoshio, and Nowacki, Werner (1966) Refinement of the crystal structure of binnite. Zeitschrift für Kristallographie, 123, 1–20.

Yates, M. G. and Ripley, E. M. (1983) Sulfur and oxygen isotope studies in the Galena mine, Coeur d'Alene district, Idaho. Geological Society of America Abstracts with Program, 15, 724.

Yund, R. A. and Kullerud, Gunnar (1966) Thermal stability of assemblages in the Cu–Fe–S system. Journal of Petrology, 7, 454–488.

Yui, Shunzo (1971) Heterogeneity within a single grain of minerals of the tennantite-tetrahedrite series. Society of Mining Geologists of Japan Special Issue, vol. 2, Proceedings of IMA-IAGOD Meeting '70, Joint Symposium Volume, 22–29.

Manuscript received, June 22, 1984;
accepted for publication, July 22, 1985.